Coordinate linkage of HIV evolution reveals regions of immunological vulnerability

Vincent Dahirel[a,b,c,1], Karthik Shekhar[a,b,1], Florencia Pereyra[a], Toshiyuki Miura[d], Mikita Artyomov[c,e], Shiv Talsania[b,f], Todd M. Allen[a], Marcus Altfeld[a], Mary Carrington[a,g], Darrell J. Irvine[a,h,i], Bruce D. Walker[a,h,2] and Arup K. Chakraborty[a,b,c,i,2]

[a]Ragon Institute of Massachusetts General Hospital, Massachusetts Institute of Technology, and Harvard University, Boston, MA 02129; Departments of [b]Chemical Engineering, [c]Chemistry, and [i]Biological Engineering, Massachusetts Institute of Technology, Cambridge, MA 02139; [e]Department of Chemistry, Moscow State University, Moscow 119991, Russia; [f]Department of Chemical Engineering, Loughborough University, Leicestershire LE11 3TU, United Kingdom; [g]Cancer and Inflammation Program, Laboratory of Experimental Immunology, SAIC-Frederick, Inc., National Cancer Institute-Frederick, Frederick, MD 21702; [h]Howard Hughes Medical Institute, Chevy Chase, MD 20815; and [d]Institute for Medical Sciences, University of Tokyo, Tokyo 108-8639, Japan

Edited* by Laurie H. Glimcher, Harvard University, Boston, MA, and approved May 20, 2011 (received for review April 4, 2011)

Cellular immune control of HIV is mediated, in part, by induction of single amino acid mutations that reduce viral fitness, but compensatory mutations limit this effect. Here, we sought to determine if higher order constraints on viral evolution exist, because some coordinately linked combinations of mutations may hurt viability. Immune targeting of multiple sites in such a multidimensionally conserved region might render the virus particularly vulnerable, because viable escape pathways would be greatly restricted. We analyzed available HIV sequences using a method from physics to reveal distinct groups of amino acids whose mutations are collectively coordinated ("HIV sectors"). From the standpoint of mutations at individual sites, one such group in Gag is as conserved as other collectively coevolving groups of sites in Gag. However, it exhibits higher order conservation indicating constraints on the viability of viral strains with multiple mutations. Mapping amino acids from this group onto protein structures shows that combined mutations likely destabilize multiprotein structural interactions critical for viral function. Persons who durably control HIV without medications preferentially target the sector in Gag predicted to be most vulnerable. By sequencing circulating viruses from these individuals, we find that individual mutations occur with similar frequency in this sector as in other targeted Gag sectors. However, multiple mutations within this sector are very rare, indicating previously unrecognized multidimensional constraints on HIV evolution. Targeting such regions with higher order evolutionary constraints provides a novel approach to immunogen design for a vaccine against HIV and other rapidly mutating viruses.

cytotoxic T-lymphocyte response | elite controllers | random matrix theory

Despite the efficacy of life-extending medications, HIV continues to wreak havoc around the world, particularly in poor nations. An efficient vaccine is urgently needed, and such a vaccine is likely to be one that induces both antibody and cytotoxic T-lymphocyte (CTL) responses (1–3). The extreme variability of the HIV envelope has precluded vaccine-induced generation of broadly neutralizing antibodies (1) that can prevent acquisition, leading some to focus on CTL-based vaccines (4) to prevent disease progression and possibly to limit acquisition (5).

CTLs recognize and respond to viral peptides presented by class I MHC proteins. Single point mutations within and surrounding such HIV epitopes targeted by CTLs can enable escape from immune pressure, leading to a focus on targeting conserved regions of the HIV proteome. Conserved regions are defined to be ones where the frequency of occurrence of mutations at single sites is small, indicating [according to evolutionary theory (6)] that the corresponding mutant viral strains are replicatively less fit. Thus, if such a site is targeted, the outgrowth of a mutant virus that escapes the immune pressure is less likely (7). The emergence of a compensatory mutation that restores fitness is a challenge to this approach (8).

Characterizing the frequency of occurrence of viral strains based on the effects of mutations at single sites results in a unidimensional measure of conservation, which ignores potential couplings between the effects of multiple simultaneous mutations due to structural/functional constraints. A useful multidimensional measure of sequence variation would be obtained if groups of sites in the viral proteome could be identified, such that sites within a group coevolve in a collectively interdependent manner to influence virus viability but each group evolves independent of other groups. If such groups exist, it is possible that a greater proportion of the combinations of mutations involving sites in the group are harmful in some groups compared with other groups. Such a group of sites is multidimensionally more conserved in that multiple mutations are more likely to hurt virus fitness and harmful combinations are less likely to be compensated for by mutations in another group (as it coevolves independently). Such regions should be particularly vulnerable to multiple points of CTL pressure, because escape pathways would be restricted. Targeting multiple points would promote the emergence of multiple mutations to escape the immune pressure, but multiple mutations in such a region would be more likely to result in unfit viruses.

Thus, we sought to determine collectively coevolving groups of residues in HIV proteins. We analyzed publicly available sequences from the Los Alamos HIV Sequence Database (http://www.hiv.lanl.gov/) of clade B HIV proteins derived from patients with diverse genotypes using random matrix theory (RMT) (9) to identify groups of sites (not pairs) that evolve collectively, presumably because they act together to perform a function important for the virus. RMT has been applied to diverse realms of physics, to analyze stock price fluctuations (10, 11), and to analyze sequences of an enzyme (12). Although inspired by Halabi et al. (12), we outline our analysis of HIV proteins by analogy with analyses of financial markets.

From price fluctuations of various stocks over time, one can compute the extent of correlation between changes in price of a pair of stocks, averaged over all available time points. This yields a matrix of pair correlations. Each element of the matrix describes correlations between a particular pair of stocks, and mathematical

Author contributions: V.D., K.S., and A.K.C. designed research; V.D., K.S., and A.K.C. performed research; F.P., T.M., M.C., and B.D.W. contributed new reagents/analytic tools; V.D., K.S., M. Artyomov, S.T., B.D.W., and A.K.C. analyzed data; and V.D., K.S., T.M.A., M. Altfeld, D.J.I., B.D.W., and A.K.C. wrote the paper.

The authors declare no conflict of interest.

*This Direct Submission article had a prearranged editor.

Freely available online through the PNAS open access option.

[1]V.D. and K.S. contributed equally to this work.

[2]To whom correspondence may be addressed. E-mail: bwalker@partners.org or arupc@mit.edu.

This article contains supporting information online at www.pnas.org/lookup/suppl/doi:10.1073/pnas.1105315108/-/DCSupplemental.

properties of the entire matrix (*Results*) reveal groups of stocks whose price fluctuations are collectively interdependent. These properties of the matrix are influenced by "noise" because of a finite sample of times and correlations that reflect changes in overall stock prices attributable to external forces (e.g., recessions). RMT has been used to "clean" the correlation matrix of these effects and obtain groups of companies whose economic activities are intrinsically collectively coupled and essentially independent of others (10, 11). Consistent with intuition, each group was composed of stocks that define known economic "sectors," such as financial service companies and automotive companies.

A similar analysis has enabled us to identify collectively coevolving groups of sites in the HIV proteome (which we term HIV sectors). Further, we have identified a sector in which mutations at multiple sites are collectively more constrained, and thus might be particularly vulnerable to multiple points of immune pressure. We examined immune targeting and sequenced circulating viruses in those rare persons who are able to control HIV without medications to determine whether such mechanisms might contribute to durable immune control. These data support our predictions. We suggest how this new understanding can be harnessed to design immunogens for a vaccine against HIV.

Results

Sequence Analysis Identifies Significant HIV Sectors. Each aligned sequence of an HIV polyprotein is analogous to stock price data at a particular time point. In a specific sequence, one asks if a mutation away from the most frequent amino acid ("wild type") at a particular position i appears simultaneously with a similar mutation at another site j, and this is done for all pairs of amino acids. Average values for the frequency of occurrence of double mutations for each pair of sites in the protein (f_{ij} for sites i and j) are obtained by repeating this procedure for all sequences (*Methods* and *SI Appendix* 1). Similarly, the frequencies with which mutations are observed at individual sites (f_i and f_j for sites i and j) are obtained. A pair correlation matrix, C, can be

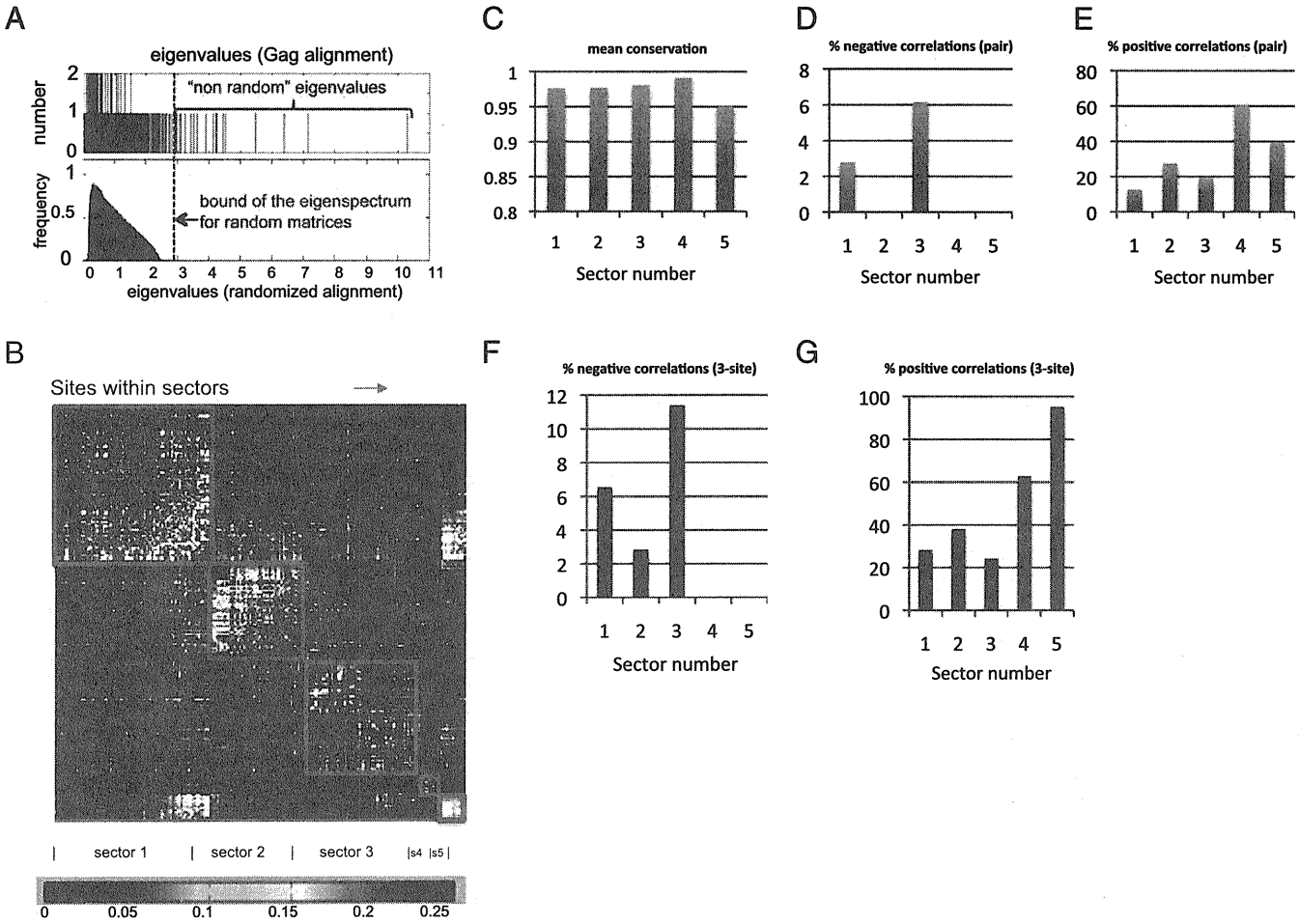

Fig. 1. Defining collectively coevolving groups of sites (sectors) in Gag. (*A, Upper*) Number of eigenvalues (ordinate) of the correlation matrix, C, for Gag (defined in the main text) with a given magnitude (abscissa) is shown. In total, 1,600 sequences of Gag polyproteins (500 residues long) were used. Note that a relatively large number of sequences of HIV proteins are available. (*Lower*) Distribution of eigenvalues obtained from 1,000 randomly generated matrices of the same size as C for Gag (described in the main text and *SI Appendix* 2). (*B*) Analyzing the eigenvectors corresponding to eigenvalues larger than the highest eigenvalue for random matrices yields collectively coevolving groups of sites or "sectors" (*SI Appendix* 3–7). Sites within a sector are grouped together along the rows and columns so that groups of collectively coevolving sites are vivid as squares along the diagonal of a heat map representing the values of the correlations (obtained from the "cleaned" correlation matrix as described in *SI Appendix* 2). (*C*) Mean frequency of the dominant amino acid at single sites within each of the five Gag sectors. (*D–F*) Threshold value defining a significant correlation was chosen to be such that correlations with magnitudes greater than this value arise with vanishing probability in the randomized matrices ($P < 0.02$). Changing this threshold value does not change qualitative results (*SI Appendix*, Fig. S11). (*D*) Percentage of significant negative ($C_{ij} < -0.03$) pair correlations within each sector. (*E*) Percentage of significant positive ($C_{ij} > 0.1$) pair correlations within each sector. (*F*) Percentage of significant three-site negative ($C_{ijk} < -0.01$) correlations within each sector (method in *SI Appendix* 17). (*G*) Percentage of significant three-site positive ($C_{ijk} > 0.1$) correlations within each sector.

defined, each element of which, C_{ij} (for sites i and j), reflects the interdependence of mutations at these two sites. $C_{ij} = (f_{ij} - f_i f_j)/\sqrt{V_i V_j}$ and measures the difference between the frequency of occurrence of a double mutant and that which would be observed if the two mutations occurred independently; the variances of the distributions of mutations (V_i and V_j) at sites i and j, respectively, normalize the values of C_{ij} for different pairs of sites. Another method (12) for computing C_{ij} yielded qualitatively similar results (*SI Appendix*, Fig. S6).

Properties of this correlation matrix, termed eigenvectors, contain information about collective coevolution of sites. Each eigenvector represents a specific combination of sites, whose mutations occur in a coupled way but are essentially independent of mutations in a combination of sites represented by another eigenvector. The data on HIV evolution can be represented as dependent on these combinations of sites (eigenvectors), rather than individual sites. The association of each site with a particular eigenvector is specified by a number that can be positive or negative. An eigenvector is also associated with a number, called an eigenvalue, whose magnitude reflects the contribution of this eigenvector to the correlations between sites (*SI Appendix*, Eq. S4).

Eigenvalues of the correlation matrix, C, for HIV Gag polyproteins are shown ordered according to their magnitudes (Fig. 1*A*, *Upper*). The corresponding eigenvectors describe groups of sites whose mutations are collectively linked, presumably by the requirements of maintaining viral fitness. However, the information in some eigenvectors is not significant because of noise (attributable to a finite sample of sequences) or because it reflects phylogeny (13).

RMT theorems can help to determine which eigenvectors reflect the influence of noise because they describe the properties of correlation matrices derived from independent random variables. For example, given the length of the Gag polyprotein and the number of available sequences, RMT states (*SI Appendix*, Eq. S3) that the largest eigenvalue would equal 2.4 if the correlation matrix reflected noise only. However, this theorem assumes that the length of the polyprotein and the number of sequences are very large. If we randomly shuffle the identity of amino acids at each site over all aligned sequences of a particular HIV protein and recalculate C, we obtain a random correlation matrix of the same size as our sample (*SI Appendix* 2). The distribution of eigenvalues obtained by randomizing the sequences 1,000 times is shown in Fig. 1*A*, *Lower*. We see that the RMT theorem is rather accurate even for finite samples, because very few eigenvalues exceed 2.4 and none exceed 3. The continuous part of the eigenvalue spectrum for the real-sequence alignment for HIV proteins is bounded in the same way as that for the randomized sequences (compare panels in Fig. 1*A* for Gag). The eigenvectors corresponding to eigenvalues <3 correspond to noise.

As noted before (12), and derived more completely in *SI Appendix* 3, the contribution of phylogeny alone to a representation of the data in terms of eigenvectors should result in an eigenvector where the contributions from each individual site in the polyprotein have the same sign. For all HIV polyproteins, the largest eigenvalue corresponds to such an eigenvector. Because each eigenvector is independent, we conclude that the eigenvector corresponding to the largest eigenvalue describes correlations attributable to phylogeny (13). Eigenvectors corresponding to the next few largest eigenvalues contain information on collective correlations between groups of sites that originate largely from relationships between evolutionary constraints and sequence.

By parsing these eigenvectors, groups of sites (sectors) in HIV proteins that coevolve together but essentially independent of others were identified. Many sites do not collectively coevolve with any other sites, and thus do not belong to any sector. For Gag, we found five strongly collectively coupled groups of sites (*SI Appendix* 6 and Fig. S4), which we term sectors 1–5. As expected, we also found an additional group of residues that is weakly coupled collectively, as a result of mutations arising in the context of specific HLA class I molecules that drive mutations at multiple sites (*SI Appendix* 8 and Figs. S4 and S5). The weakly collective linkage between this group of sites is attributable to HLA-associated "footprints" [i.e., these mutations arise in persons with the same HLA type (14)]; thus, we do not consider this quasi-sector further.

Gag sectors 1–5 can be visualized as a heat map reflecting the correlations between sites (Fig. 1*B*). As expected, the sites that comprise a sector are not contiguous along the linear protein sequence. The positions of the sites along the rows and columns in Fig. 1*B* group the sites in a sector together. For example, if a sector was composed of sites 27, 45, and 53 along the linear protein sequence, these sites would be adjacent to each other along a row or column. Each group of sites that comprises a sector is outlined in red. We observed similar groupings for other HIV proteins (*SI Appendix*, Figs. S7–S10). We focus further analysis on Gag because of data indicating correlations between Gag-specific responses and viral control (15) and a strong impact of Gag mutations on viral fitness (16).

Identification of an Immunologically Vulnerable Sector in Gag. From the standpoint of identifying regions with single sites that are more conserved, all five Gag sectors are equivalent (Fig. 1*C*). However, if one examines the relative occurrence of positive and negative correlations between multiple mutations at sites that comprise each collectively evolving sector, differences between the sectors become apparent.

Negative correlation between sites implies that the multiple mutant is observed less frequently than if the individual mutations were to arise independently. For example, consider a simple case where a pair of sites (i and j) is negatively correlated, with each site being 90% conserved [i.e., the frequency with which single mutations at sites i and j are observed is 10%, ($f_i = f_j = 0.1$)]. For C_{ij} (proportional to $f_{ij} - f_i f_j$) to be negative, the frequency with which the double mutant is observed (f_{ij}) must be less than 1%. This implies that when multiple sites are negatively correlated, the multiple mutant is considerably less fit compared with the single mutants. If immune pressure is applied to multiple sites in a sector, escaping the immune pressure is likely to require more than one mutation. The greater the proportion of negative correlations in the sector, the more difficult it is to both escape the CTL pressure and maintain virus fitness, because multiple mutations are much less tolerated, likely because of fitness limitations.

Positive correlation between sites implies that the corresponding multiple mutants are observed more frequently than if the mutations were to occur independently. Thus, positive correlations can be associated with compensatory mutations; indeed, known compensatory mutations do appear as positive correlations (*SI Appendix*, Table S9). Thus, sectors characterized by larger numbers of positive correlations would be less effective targets, because escape from CTLs without substantial loss in virus fitness is more likely.

For pairs of sites within a sector, one finds that Gag sector 3 contains the largest proportion of negative correlations compared with other sectors and a relatively small number of positive correlations (Fig. 1 *D* and *E*). This is also true for three-site (Fig. 1 *F* and *G*) and higher order correlations. The magnitudes of the negative pair correlations between sites in sector 3 are as large as they can be, given the level of single site conservation in this sector (details in *SI Appendix* 11), meaning that the double mutants are expected to be observed very rarely. The eigenmaps in *SI Appendix*, Fig. S4 *B* and *C* also show that several sites in sector 3 are collectively (i.e., at higher order) negatively correlated to several others, which is not true for other sectors. Note that we do not identify important negative pair correlations by screening all pair correlations for those that exceed a cutoff (17). Rather, we first identified groups of sites (sectors) that are significantly collectively coupled (because RMT theorems help to eliminate noise-induced

correlations). We then examined the signs of multibody correlations only within these meaningful collectively coupled sectors.

Our results suggest that sector 3 is the most immunologically vulnerable multidimensionally constrained region in Gag, because multiple mutations are most constrained in this sector. Because sequence analysis methods are not exact, we tested this prediction, and its consequences for HIV infection and vaccination, against existing and new experimental data.

Sector 3 Is Immunologically Vulnerable Because of the Importance of Assembling Multiprotein Structures Critical for Viral Capsid Formation. In sector 3, 52 of the 57 sites are contained in the p24 protein but their locations within an individual p24 protein appear random (Fig. 2*A*; individual amino acids in *SI Appendix*, Table S1). However, hexamers of the p24 protein form the viral capsid (18), and superimposing sector 3 sites on the structure of the p24 hexamer (19) shows that the preponderance of these sites (~68%) is at interfaces between p24 proteins in a hexamer or at interfaces between the hexamers that form the capsid (Fig. 2*B*). Coevolution of this group of sites originates from constraints important for assembly of functional multiprotein structures, highlighting the importance of determining collective correlations.

The structural locations of sector 3 sites suggest the origin of negative correlations. Whereas one mutation in interface residues may still allow formation of p24 hexamers and assembly of the hexamers to form the viral capsid, multiple simultaneous mutations would likely destabilize these protein-protein interfaces. Fitness cost predictions of multiple mutations in sector 3, and comparisons with available data (20), are included in *SI Appendix*, Table S9–S11.

Sector 1 sites also reflect structural constraints associated with supramolecular assembly because they largely comprise the core of the hexamer (Fig. 2*C*). However, our analyses suggest that sector 1 is not as immunologically vulnerable as sector 3. This is because of the following:

i) The ratio of negative to positive correlations for pairs of mutations is a factor of 3 greater for sector 3.
ii) At the level of three-site correlations, the ratio of negative to positive correlations is more than threefold greater for sector 3.
iii) Sector 3 is characterized by collective higher order negative correlations between sites that are absent in sector 1 (*SI Appendix*, Fig. S4).

These results may be because multiple mutations in sector 3 residues result in disruption of intra- and interhexamer interfaces, whereas mutations in the core of the hexamer are less likely to disrupt virion assembly (21).

Elite Controllers of HIV Preferentially Target Multiple Sites in Sector 3. Our results suggest that applying CTL pressure at multiple sites contained in sector 3 is likely to facilitate durable control of viral load to low levels; multiple mutations that allow immune escape are more likely to hurt viral fitness significantly, because multidimensional escape pathways are restricted. Can HLA (human MHC class I) molecules present peptides containing multiple sites within the identified vulnerable region? Because elite controllers achieve viral control (16), we first analyzed the locations of sites contained in peptides targeted in individuals with HLA alleles associated with spontaneous HIV control (HLA-A*25, B*57, B*27, B*14, Cw*08) (22). Remarkably, the sector with the largest proportion of sites contained in the dominant peptides targeted by controllers is sector 3 ($P = 3{\cdot}10^{-7}$; Fig. 3*A* and *SI Appendix*, Table S3). CTL pressure imposed by individuals with these HLA alleles, however, is not the driver of this collectively coevolving group of sites for reasons that include:

i) There are clear structural explanations (Fig. 2) for the collective correlations that characterize sector 3 sites, and structural features are independent of immune pressure.
ii) Negative correlations cannot be induced by immune pressure, because mutations induced in persons with the same HLA would be more likely to arise than if they occurred independently.
iii) As noted, a quasi-sector describes weak correlations associated with HLA-associated mutations (*SI Appendix*, Fig. S5), and these sites are not a part of sector 3.

Thus, the sector we identify to be most vulnerable by analyses of viral sequences and supramolecular structures is the most targeted by controllers.

Examining targeted epitopes lends further insights. For example, eight amino acids in the dominant epitopes targeted by B57-restricted CTLs are in sector 3; this multiplicity is further augmented by the enhanced cross-reactivity of these CTLs (23). $B14^+$ individuals target three amino acids in this sector. Population studies indicate that HLA-$B57^+$/$B14^+$ persons are partic-

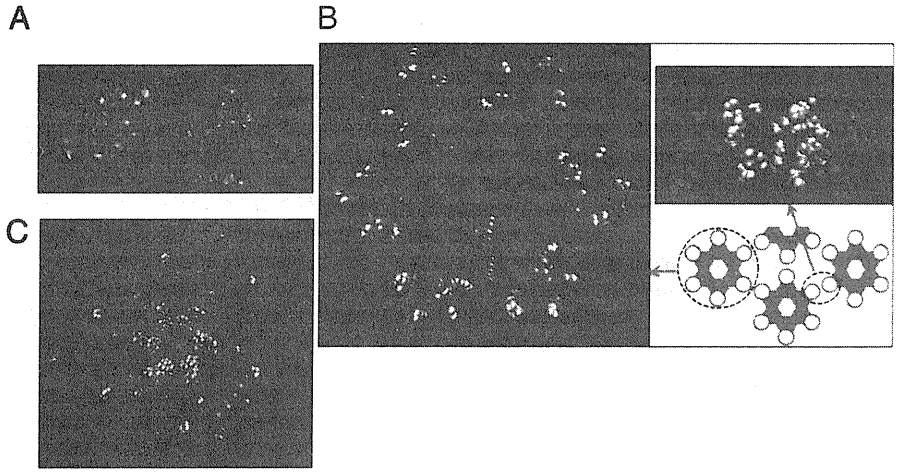

Fig. 2. Protein structures reveal the origin of collective correlations. (*A*) Sector 3 sites represented on the structure of the p24 monomer (PDB ID code 3GV2) are shown as purple spheres. (*B*) Sector 3 sites represented on the structure of the p24 hexamer (PDB code 3GV2) and the structure of the interface between hexamers (PDB code 2KOD). Sites at interfaces between two p24 proteins belonging to two adjacent hexamers are shown in green, and sites at interfaces between two p24 molecules within a hexamer are shown in red. The few remaining sites in sector 3 that are not part of these interfaces are shown in purple. (*C*) Sector 1 sites are shown in cyan on the structure of the p24 hexamer.

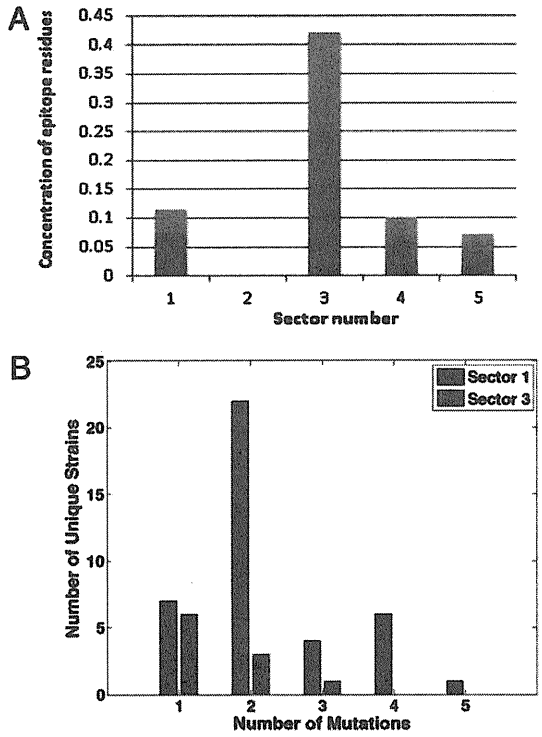

Fig. 3. Concentration of sites from the dominant epitopes presented by elite controllers in each sector and comparison of mutation patterns in sectors 1 and 3 in viruses derived from elite controllers. (*A*) Epitope is defined as dominant if it is the most targeted (in Gag) by individuals with the corresponding HLA allele. Concentration is the number of epitope sites in the sector divided by the total number of residues in the sector. The *P* value of association with each sector is in *SI Appendix* 10. Only sector 3 is significantly enriched with sites from the dominant epitopes of HLA molecules associated with control. Sectors 4 and 5 are not targeted at multiple points because they contain only 10 and 14 sites, respectively. Sectors 1 and 3 are targeted at multiple points. (*B*) Comparison of the number of unique viral strains obtained from a cohort of elite controllers that contains different numbers of mutations in sectors 1 and 3.

ularly efficient controllers of HIV infection. Our results suggest that this is because viral strains that can escape the multiple points of immune pressure in this sector are likely to have very low fitness. Thus, point mutants with lower viral fitness that only partially escape immune pressure or strains with multiple mutations that are not negatively correlated are likely to be the only options for the virus. This is consistent with the observed lower viral load and lower average viral fitness in controllers (16). Note also that CTLs restricted by HLA molecules associated with progression do not target sector 3 sites significantly ($P = 0.37$; *SI Appendix*, Table S3).

Virus Sequences from Patients Show That Multiple Mutations in Sector 3 Are Unlikely. Roughly 10% of sites in sectors 1, 4, and 5 are targeted by controllers, and sector 2 is not targeted (Fig. 3*A*). However, because sectors 4 and 5 are composed of only 10 and 14 sites, respectively, only 1 site (and epitope) is targeted by controllers in these sectors. Because sector 1 comprises 79 sites, many sites in sector 1 are targeted by controllers. If two regions of the proteome are equally targeted, all things being equal, the number and types of mutations observed in these regions should be similar. Sectors 1 and 3, both in Gag, exhibit similar levels of single site conservation, but we find that sector 3 is more multidimensionally constrained. Thus, we predict that even though sector 3 is targeted more than sector 1, fewer HIV strains with multiple mutations in sector 3 sites would be viable compared with those with similar mutations in sector 1.

To test this prediction, we sequenced viruses obtained from elite controllers because they target both sectors 1 and 3. We obtained 72 sequences from plasma and 103 including both plasma and peripheral blood mononuclear cells (PBMCs). The qualitative results obtained from analyzing either set of sequences are the same (Fig. 3*B* and *SI Appendix* 18). As per our predictions, the frequency of single mutations in sectors 1 and 3 is similar but multiple mutations are significantly rarer in sites that comprise sector 3. Our results suggest that this is because viral strains that can escape multiple points of immune pressure in sector 3 are more likely to be associated with negative correlations, and hence have particularly low replicative fitness because of defective capsid assembly. Thus, they are unlikely to be viable, and we do not observe them. These results show that the calculated differences between collective correlations among sites that comprise sector 3 and other sectors (Fig. 1) result in qualitative differences in viral mutations observed in humans that target sector 3 sites. Note also that almost all the few viral strains that we observe with multiple mutations in sector 3 are associated with positive correlations (*SI Appendix*, Fig. S13). Although only positive correlations can correspond to compensatory mutations, positive correlations can also correspond to multiple mutants that are only moderately less fit compared with single mutants, unlike negative correlations, which are only associated with multiple mutants that are very deleterious.

Our results strongly support our hypothesis that applying CTL pressure at multiple points in a multidimensionally constrained group of sites can trap the virus, because we find that controllers target multiple sites in sector 3, but strains with multiple mutations in sector 3 are not viable. Thus, viable strains are still likely to be subject to immune pressure.

Immunogens That May Induce CTL Responses in a Population That Hurt HIV. Can such potent responses be induced by vaccination in persons who are not blessed with HLA alleles that mount the correct dominant responses? Individuals with other HLA alleles present subdominant peptides containing sites in the vulnerable regions we have identified (using the Epitope Tables of the Los Alamos HIV Molecular Immunology Database, http://www.hiv.lanl.gov/content/immunology/tables/tables.html). This suggests the following strategy for design of immunogens that could induce memory CTL responses targeting the most vulnerable regions of HIV in a population: Select protein segments that simultaneously maximize sites in sector 3 (and some sites in sector 1), which are characterized by negative correlations, and those contained in subdominant and dominant epitopes presented by HLA molecules that span a broad section of a population. Such immunogens should elicit memory CTLs that only target the multidimensionally conserved regions of HIV, because epitopes that are dominantly targeted ineffectually are excluded. During natural infection, these memory CTLs are expected to mount robust responses that hit HIV where it hurts early, before naive CTLs mount ineffective dominant responses. Mounting the right responses early is important for HIV infections (2), because there is a short window of time before the immune system is compromised.

To illustrate this strategy, we considered a target population, white Americans with the 25 most frequent haplotypes (~39% of this population) (24). We create all groups of 10 known epitopes (as an example) presented by HLA-A/B molecules that comprise these haplotypes and select the top 10 groups according to the two criteria noted above (*SI Appendix* 12). One top-scoring immunogen (p24 residues 160–188 and 240–277) contains at least 1 or 2 targeted epitopes in 97% and 56% of the target population, respectively (a lower bound, because many epitopes are unknown). Previous empirical data show that controllers target p24 sites 240–272 (25). Sites 160–188 contain only 1 epitope tar-

geted by known controllers but represent an equally vulnerable region that provides broad coverage.

Discussion

Immunogens designed in this way to include only the multidimensionally constrained regions of the HIV proteome, which also contain epitopes presented by diverse HLAs in a population, are candidates for peptide vaccines using synthetic vectors (26), or by linking each segment together, they can be analogs of mosaic immunogens (27) delivered by traditional vectors. Such an immunogen would target the most vulnerable regions of HIV rather than the whole proteome. Targeting the latter is more likely to elicit responses from which HIV can escape via mutations (28), while hindering a focused response directed at regions of immunological vulnerability we have identified. Our goal of identifying such regions, and the methods we have used toward this end, are different from previous efforts to study coevolution of HIV proteins (e.g., 14, 29–31). Further analysis following the logic described by us should reveal additional regions of HIV proteins that are multidimensionally constrained, thereby enhancing the list of regions that are candidates for inclusion in a potent vaccine. A practical vaccine may also require inclusion of CD4 epitopes and flanking residues needed for antigen processing which do not contain protein segments that are likely to elicit ineffectual memory CTL responses. In vitro experiments and studies with animal models are required to develop this new concept, which might also be applied to design efficacious immunogens against other viruses. Our results also suggest the design of new small-molecule inhibitors of HIV replication.

Methods

HIV Sequences and Similarity Analysis. Multiple sequence alignments of nucleotide sequences of HIV-1 Gag, RT, and Nef were downloaded from the Los Alamos HIV Sequence Database (http://www.hiv.lanl.gov/) (clade B, one sequence per patient). We checked the phylogenetic homogeneity of each set by performing a principal component analysis of the similarity matrix of sequences (*SI Appendix* 5).

Identification of HIV Sectors. The correlation matrix for a given set of sequences is cleaned from phylogeny and noise using RMT (as described in the main text and *SI Appendix* 1–4). The definition of sectors follows the strategy proposed by Halabi et al. (12), grouping positions with a particular spectral signature into a sector (*SI Appendix* 6).

Targeting by Elite Controllers. We defined a set of epitopes dominantly targeted by HLA alleles associated with control (22), using a published dataset of the frequency of recognition of epitopes in an HLA-specific population (32).

Sequencing Viruses from Elite Controllers. HIV-1 Gag was amplified using nested RT-PCR from previously frozen PBMCs or plasma from elite controllers as previously described (33). PCR products were purified, and cycle-sequencing reactions were performed using 60 HIV-1–specific sequencing primers. Population sequences were obtained using an ABI 3730 PRISM (Applied Biosystems) automated sequencer. Gag mutations in the sequences derived from elite controllers were defined with reference to the clade B consensus sequence.

ACKNOWLEDGMENTS. We thank D. Barouch and H. Eisen for valuable discussions. Financial support was provided by the Ragon Institute, a National Institutes of Health Director's Pioneer Award (to A.K.C.), National Institutes of Health Grants RO130914 (to B.D.W.) and PO1 AI074415 (to M. Altfeld and T.M.A.), The Howard Hughes Medical Institute (B.D.W.) and the Mark and Lisa Schwartz Foundation (B.D.W.) This project has been funded in whole or in part with federal funds from the National Cancer Institute, National Institutes of Health, under Contract HHSN261200800001E.

1. Walker BD, Burton DR (2008) Toward an AIDS vaccine. *Science* 320:760–764.
2. McMichael AJ, Borrow P, Tomaras GD, Goonetilleke N, Haynes BF (2010) The immune response during acute HIV-1 infection: Clues for vaccine development. *Nat Rev Immunol* 10:11–23.
3. Amanna IJ, Slifka MK (2011) Contributions of humoral and cellular immunity to vaccine-induced protection in humans. *Virology* 411:206–215.
4. Barouch DH, Korber B (2010) HIV-1 vaccine development after STEP. *Annu Rev Med* 61:153–167.
5. Hansen SG, et al. (2009) Effector memory T cell responses are associated with protection of rhesus monkeys from mucosal simian immunodeficiency virus challenge. *Nat Med* 15:293–299.
6. Hartl DL, Clark AG (2007) *Principles of Population Genetics* (Sinauer, Sunderland, MA), 4th Ed.
7. Altfeld M, Allen TM (2006) Hitting HIV where it hurts: An alternative approach to HIV vaccine design. *Trends Immunol* 27:504–510.
8. Goulder PJ, Watkins DI (2004) HIV and SIV CTL escape: Implications for vaccine design. *Nat Rev Immunol* 4:630–640.
9. Wigner EP (1967) Random matrices in physics. *SIAM Rev* 9:1–23.
10. Plerou V, et al. (2002) Random matrix approach to cross correlations in financial data. *Phys Rev E Stat Nonlin Soft Matter Phys* 65:066126.
11. Laloux L, Cizeau P, Bouchaud JP, Potters M (1999) Noise dressing of financial correlation matrices. *Phys Rev Lett* 83:1467–1470.
12. Halabi N, Rivoire O, Leibler S, Ranganathan R (2009) Protein sectors: Evolutionary units of three-dimensional structure. *Cell* 138:774–786.
13. Bhattacharya T, et al. (2007) Founder effects in the assessment of HIV polymorphisms and HLA allele associations. *Science* 315:1583–1586.
14. Brumme ZL, et al. (2009) HLA-associated immune escape pathways in HIV-1 subtype B Gag, Pol and Nef proteins. *PLoS ONE* 4:e6687.
15. Kiepiela P, et al. (2007) CD8+ T-cell responses to different HIV proteins have discordant associations with viral load. *Nat Med* 13:46–53.
16. Miura T, et al. (2009) HLA-associated viral mutations are common in human immunodeficiency virus type 1 elite controllers. *J Virol* 83:3407–3412.
17. Hoffman NG, Schiffer CA, Swanstrom R (2003) Covariation of amino acid positions in HIV-1 protease. *Virology* 314:536–548.
18. Ganser-Pornillos BK, Yeager M, Sundquist WI (2008) The structural biology of HIV assembly. *Curr Opin Struct Biol* 18:203–217.
19. Pornillos O, et al. (2009) X-ray structures of the hexameric building block of the HIV capsid. *Cell* 137:1282–1292.
20. Troyer RM, et al. (2009) Variable fitness impact of HIV-1 escape mutations to cytotoxic T lymphocyte (CTL) response. *PLoS Pathog* 5:e1000365.
21. Adamson CS, Jones IM (2004) The molecular basis of HIV capsid assembly—Five years of progress. *Rev Med Virol* 14:107–121.
22. Pereyra F, et al.; International HIV Controllers Study (2010) The major genetic determinants of HIV-1 control affect HLA class I peptide presentation. *Science* 330: 1551–1557.
23. Kosmrlj A, et al. (2010) Effects of thymic selection of the T-cell repertoire on HLA class I-associated control of HIV infection. *Nature* 465:350–354.
24. Maiers M, Gragert L, Klitz W (2007) High-resolution HLA alleles and haplotypes in the United States population. *Hum Immunol* 68:779–788.
25. Streeck H, et al. (2007) Recognition of a defined region within p24 gag by CD8+ T cells during primary human immunodeficiency virus type 1 infection in individuals expressing protective HLA class I alleles. *J Virol* 81:7725–7731.
26. Melief CJ, van der Burg SH (2008) Immunotherapy of established (pre)malignant disease by synthetic long peptide vaccines. *Nat Rev Cancer* 8:351–360.
27. Barouch DH, et al. (2010) Mosaic HIV-1 vaccines expand the breadth and depth of cellular immune responses in rhesus monkeys. *Nat Med* 16:319–323.
28. Altfeld M, Goulder PJ (2011) The STEP study provides a hint that vaccine induction of the right CD8+ T cell responses can facilitate immune control of HIV. *J Infect Dis* 203: 753–755.
29. Liu Y, Eyal E, Bahar I (2008) Analysis of correlated mutations in HIV-1 protease using spectral clustering. *Bioinformatics* 24:1243–1250.
30. Fares MA, Travers SAA (2006) A novel method for detecting intramolecular coevolution: adding a further dimension to selective constraints analyses. *Genetics* 173:9–23.
31. Bickel PJ, et al. (1996) Covariability of V3 loop amino acids. *AIDS Research and Human Retroviruses* 12:1401–1411.
32. Streeck H, et al. (2009) Human immunodeficiency virus type 1-specific CD8+ T-cell responses during primary infection are major determinants of the viral set point and loss of CD4+ T cells. *J Virol* 83:7641–7648.
33. Miura T, et al. (2008) Genetic characterization of human immunodeficiency virus type 1 in elite controllers: Lack of gross genetic defects or common amino acid changes. *J Virol* 82:8422–8430.

AIDS RESEARCH AND HUMAN RETROVIRUSES
Volume 27, Number 00, 2011

DOI: 10.1089/aid.2011.0073

Imbalanced Production of Cytokines by T Cells Associates with the Activation/Exhaustion Status of Memory T Cells in Chronic HIV Type 1 Infection

Kaori Nakayama,[1] Hitomi Nakamura,[2] Michiko Koga,[2] Tomohiko Koibuchi,[2] Takeshi Fujii,[2] Toshiyuki Miura,[1] Aikichi Iwamoto,[1,2] and Ai Kawana-Tachikawa[1]

Abstract

Chronic HIV-1 infection is characterized by immune cell dysfunctions driven by chronic immune activation. Plasma HIV-1 viral load (VL) is closely correlated with disease progression and the level of immune activation. However, the mechanism by which the persistent presence of HIV-1 damages immune cells is still not fully understood. To evaluate how HIV-1 affects disruption of T cell-mediated immune responses during chronic HIV-1 infection we determined the functional profiles of T cells from subjects with chronic HIV-1 infection. We measured the capacity of peripheral blood mononuclear cells (PBMCs) to produce 25 specific cytokines in response to nonspecific T cell stimulation, and found that the capacity to produce Th-1-related cytokines (MIP-1α, MIP-1β, RANTES, IFN-γ, and MIG), sIL-2R, and IL-17, but not Th-2-related cytokines, was inversely correlated with plasma VL. The capacities to produce these cytokines were interrelated; notably, IL-17 production had a strong direct correlation with production of MIP-1α, MIP-1β, RANTES, and IFN-γ. In both $CD4^+$ and $CD8^+$ T cells, dysfunctional production of cytokines was associated with T cell activation (CD38 expression) and exhaustion (PD-1 and/or CTLA-4 expression) status of memory subsets. Although the capacity to produce these cytokines was recovered soon after multiple $\log_{10}$ reduction of plasma viral levels by antiretroviral therapy, memory $CD8^+$ T cells remained activated and exhausted after prolonged virus suppression. Our data suggest that HIV-1 levels directly affect the ability of memory T cells to produce specifically Th1- and Th17-related cytokines during chronic HIV-1 infection.

Introduction

PLASMA VIRAL LOAD (VL) and CD4-positive T cell count are two surrogate markers of HIV-1 disease progression.[1] Throughout the course of infection both innate and adaptive immune systems are highly activated, and disease progression is strongly correlated with immune activation status.[2,3] Notably, immune activation is observed in both HIV-1 and pathogenic SIV infection, but not in nonpathogenic SIV infection in a natural host.[4,5] Moreover, studies have shown that T cells in patients with high VL and progressive disease are less functional, have less proliferative capacity, and are more exhausted than T cells in patients with low VL and slow disease progression.[6–12] In those patients, exhaustion is seen not only in HIV-1-specific T cells, but also in nonspecific T cells.[11,13] These data suggest that immune cells have lost their original function due to persistent hyperactivation, which depends on VL, during chronic HIV-1 infection.

The immune system is highly coordinated: the cytokine network regulates interactions between cells, and cytokine balance dictates how the immune system responds. Cytokine production determines the specific helper functions of $CD4^+$ T cells and allows balance in immune responses *in vivo*.[14–16] A possible explanation of the impaired immune response in chronic HIV-1 infection is that the ability of T cells to balance cytokine production has been altered, just as alteration of balance between Th1- and Th2-type immune response affects the clinical course of certain infectious diseases and autoimmune syndromes.[17,18]

To evaluate T cell impairment resulting from persistent immune activation during chronic HIV-1 infection, we compared the cytokine expression spectra of peripheral blood mononuclear cells (PBMCs) in response to nonspecific T cell stimulation in treatment-naive HIV-1-infected subjects with low or high VL. We also examined the differentiation states and activation levels of $CD4^+$ and $CD8^+$ T cells from

[1]Division of Infectious Diseases, Advanced Clinical Research Center, and [2]Department of Infectious Diseases and Applied Immunology, Research Hospital, The Institute of Medical Science, The University of Tokyo, Tokyo, Japan.

HIV-1-infected subjects to elucidate relationships between cytokine expression capacity and T cell phenotypic status.

Materials and Methods

Study design

HIV-1-infected individuals who were under medical supervision at our clinic were asked to provide blood samples for this study. Blood samples were taken from selected patients in the chronic phase of HIV-1 infection, with CD4 counts >200 cells/ml. We requested blood samples from antiretroviral therapy (ART)-naive patients with either low plasma viral load (VL) values (<5000 copies/ml; LVL group) or high VL values (>25,000 copies/ml; HVL group), and from treatment-experienced patients who had received ART >2 years (Tx group). Blood samples were also obtained from a small number of HIV-1-infected patients who had first initiated ART within the previous 1–2 months. As controls, blood samples were obtained from HIV-1-seronegative individuals (healthy controls; HC).

All participants gave written informed consent, and the study was approved by the institutional review boards of the Institute of the Medical Science of the University of Tokyo (No. 11-2-0329 and 20-47-210521).

PBMC cultures and PHA stimulation

PBMCs were isolated from heparinized whole blood by Ficoll-Paque PLUS density gradients (GE Healthcare, Piscataway, NJ) and cryopreserved in liquid nitrogen until use. The frozen cells were thawed 1 day before stimulation and cultured in R10 medium [RPMI 1640 medium (Sigma, St. Louis, MO) supplemented with 10% heat-inactivated fetal calf serum (FCS; Sigma), 100 U penicillin/ml, 100 μg/ml streptomycin (Sigma), 2 mmol/liter L-glutamine (Sigma), and 10 mmol/liter 4-(2-hydroxyethyl)-1-piperazineethanesulfonic acid (HEPES; Sigma)] at 37°C, 5% CO_2. The following day 5×10^5 cells/well were cultured in 250 μl/well of R10 medium with or without 2 μg/ml phytohemagglutinin L (PHA; Roche Applied Science, Mannheim, Germany). Culture supernatants were harvested after 48 h and stored at −80°C until use for multiple cytokine assays.

Quantification of cytokines

The human cytokine 25-plex antibody kit (Invitrogen Corporation, Carlsbad, CA) was used to measure the levels of 25 cytokines in culture supernatants: interleukin (IL)-1 receptor antagonist protein (IL-1RA), IL-1β, IL-2, soluble IL-2R (sIL-2R), IL-4, IL-5, IL-6, IL-7, IL-8, IL-10, IL-12p40/70, IL-13, IL-15, IL-17, eotaxin, interferon gamma (IFN-γ)-induced protein 10 kDa (IP-10), monocyte chemoattractant protein-1 (MCP-1), monokine induced by IFN-γ (MIG), macrophage inflammatory protein 1alpha (MIP-1α), MIP-1β, regulated on activation normal T cell expressed and secreted (RANTES), tumor necrosis factor-α (TNF-α), granulocyte-macrophage colony-stimulating factor (GM-CSF), IFN-α, and IFN-γ. The detection limits for the cytokines measured by the kit were as follows: IL-5, IL-6, IL-8, 3 pg/ml; MIG, 4 pg/ml; IL-4, IL-10, IFN-γ, IP-10, eotaxin, 5 pg/ml; IL-2, 6 pg/ml; IL-7, IL-13, IL-15, IL-17, TNF-α, MIP-1α, MIP-1β, MCP-1, 10 pg/ml; IL-1β, IL-12p40/70, IFN-α, GM-CSF, RANTES, 15 pg/ml; IL-1RA, sIL-2R, 30 pg/ml. As the amounts of IL-6, IL-8, TNF-α, MIP-1α, MIP-1β, IP-10, MIG, and MCP-1 produced from PHA-stimulated PBMCs were beyond the range of the assay, we diluted the samples 10-fold prior to measurement of these cytokines. However, IL-8 levels were out of range in most patient samples and could not be measured accurately.

Samples were loaded onto the Luminex100 system (Luminex Corporation, Austin, YX), and samples were quantified by analysis of the median fluorescence intensity of the beads using MasterPlex QT version 2.5 (Luminex Corporation). The assays were performed according to the manufacturer's instructions, and all samples were run in duplicate.

Identification of cytokine-producing cells in PBMCs

$CD14^+$ cells (monocytes), $CD8^+$ T cells, $CD4^+$ T cells, and $CD56^+CD16^+$ (NK) cells were isolated sequentially from PBMCs of each healthy subject. Magnetic cell separation (MACS) selection was performed using anti-CD14, anti-CD8, and anti-CD4 antibody-conjugated microbeads or using the $CD56^+CD16^+$ NK cell isolation kit (Miltenyi Biotic, Bergisch Gladbach, Germany). The purity of each cell fraction was >95% as determined by flow cytometry.

Fractionated cells were cultured separately or were co-cultured in the presence of 2 μg/ml PHA at 37°C, 5% CO_2, for 48 h. Levels of MIP-1α, MIP-1β, RANTES, IL-2R, IFN-γ, and IL-17 in culture supernatants were measured with DuoSet ELISA Development Systems (R&D Systems). The absolute numbers of each cell fraction used in the experiments were calculated from the average proportion of each subset in PBMCs.

Antibodies

The fluorochrome-conjugated monoclonal antibodies (mAb) used in the study were as follows: fluorescein isothiocyanate (FITC)-labeled anti-MIP-1α, anti-MIP-1β, and anti-RANTES (R&D Systems, Minneapolis, MN); FITC-labeled anti-PD-1 and anti-Ki67, phycoerythrin (PE)-labeled anti-Bcl-2, peridinin cholorophyll protein/cyanin5.5 (PerCP Cy5.5)-labeled anti-CD38 and anti-CD3, PE Cy7-labeled anti-CCR7, allophycocyanin (APC)-labeled anti-CD45RA, and pacific blue-labeled anti-CD4 (BD Biosciences, San Jose, CA); APC AlexaFluor 750-labeled anti-CD4, pacific blue-labeled anti-IFN-γ, and AlexaFluor 647-labeled anti-IL-17A (eBioscience, San Diego, CA); PE-labeled anti-IL-4 (Becton Dickinson, Franklin Lakes, NJ); APC Cy7-labeled anti-CD3 (BioLegend, San Diego, CA); and Pacific Orange-labeled anti-CD8 (Invitrogen).

Surface phenotypic and intracellular cytokine staining

For intracellular cytokine staining, cryopreserved PBMCs were thawed and cultured in R10 overnight. The following day cells were stimulated with phorbol ester (PMA)/calcium ionophore (ionomycin) in the presence of Golgi inhibitor (brefeldin A) for 5 h. Cells were stained with a panel of fluorescently labeled antibodies against cell-surface markers. For detection of dead cells, the cells were also stained with 5 μg/ml ethidium monoazide bromide (EMA; Sigma). Cells were washed twice and exposed to fluorescent light for 10 min on ice to allow the EMA to bind to DNA in dead cells. Cells were then fixed in 2% paraformaldehyde and permeabilized in BD FACS Permeabilizing Solution 2 (BD Biosciences) prior to antibody staining for intracellular molecules.

Dead or dying cells were detected by surface phenotypic staining with propidium iodide (PI; Sigma).

Flow cytometric analysis

Samples were analyzed on a FACSAria multilaser cytometer (Beckton Dickinson) running FACSDiva software, with collections of 60,000–100,000 lymphocyte-gated events. Data were analyzed with FlowJo software (Tree Star, Ashland, OR).

Statistical analysis

GraphPad Prism5 software (San Diego, CA) was used for all statistical analysis. Differences between groups were tested for statistical significance using the nonparametric Mann–Whitney *U* test. Since previous studies revealed that production of multiple cytokines by HIV-specific T cells was limited in progressors compared to nonprogressors,[6,19] the production levels of cytokines were expected to differ among LVL, HVL, and healthy control subjects. For this reason, we did not consider multiple comparison correction for Mann–Whitney *U* tests to avoid false-negative results. Correlation analysis was performed using Spearman's rank correlation. The level of significance for all analyses was set at $p < 0.05$.

Results

Study population

Most analyses were performed using blood samples collected from 35 HIV-1-infected, ART-naïve patients, 15 HIV-1-infected, treatment-experienced patients, and 16 HIV-1-seronegative individuals. Demographic characteristics of these 50 HIV-1-infected patients are presented in Table 1. The 35 HIV-1-infected, ART-naive patients included 19 patients with low VL (LVL group; median VL: 1200, range: 53 to 3600) and 16 patients with high VL (HVL group; median VL: 62,000; range: 25,000 to 500,000). The median CD4 counts in the LVL and HVL groups were 449 (range: 316 to 749) and 407 (range: 228 to 520), respectively; the difference was not statistically significant. The groups also showed no significant difference in age, another factor that influences immune status.

The 15 HIV-1-infected individuals recruited into the study to represent treatment-experienced patients had received ART and successfully controlled their disease over a long period of time (median: 66 months; range: 22 to 149 months). To examine the impact of actively decreasing VL on the functional profile of PBMCs, blood samples were also collected from six HIV-1-infected patients who had initiated treatment only in the previous 1–2 months.

Cytokine production in PHA-stimulated PBMCs

Cytokine measurements from cells cultured for 48 h in an unstimulated state were at the limit of detection (data not shown). We initially compared anti-CD3-antibody and PHA as a nonspecific stimulus of PBMCs to induce cytokine production, and found that the production levels of most cytokines were much higher in PHA-stimulated PBMCs than in anti-CD3-antibody-stimulated PBMCs (data not shown). When cells were stimulated with PHA and cultured for 48 h, production of most cytokines increased dramatically (Fig. 1A). There were no significant differences between any groups in IL-2, IL-13, IL-15, IL-1β, IFN-α, TNF-α, eotaxin, or IP-10 production (data not shown).

Cytokine production in PBMCs from treatment-naive HIV-1 subjects was compared to cytokine production in PBMCs from healthy control subjects. Median levels of many cytokines in the HVL group were significantly different from those in the healthy control group: MIP-1α [6.33 (range 0.99–21.01) vs. 16.92 (10.36–23.87) ng/ml; $p = 0.0005$], MIP-1β [8.51 (1.37–26.42) vs. 21.44 (10.26–34.11) ng/ml; $p = 0.0036$], IFN-γ [1.50 (0.30–5.75) vs. 2.64 (0.79–5.78) ng/ml; $p = 0.0402$], IL-7 [<0.01 (<0.01–0.67) vs. 0.04 (<0.01–0.07) ng/ml; $p = 0.0077$], IL-1Ra [18.93 (0.59–27.61) vs. 1.50 (0.55–14.95) ng/ml; $p = 0.0184$], IL-6 [0.63 (0.11–12.23) vs. 1.77 (0.68–4.93) ng/ml; $p = 0.0254$], and IL-10 [0.08 (<0.005–0.40) vs. 0.55 (0.13–0.83) ng/ml; $p = 0.0031$]. In contrast, significant differences between the LVL group and the healthy control group were seen only in levels of IL-10 [0.12 (<0.005–0.72) vs. 0.55 (0.13–0.83) ng/ml; $p = 0.0050$] and IL-1Ra [17.05 (0.49–28.31) vs. 1.50 (0.55–14.95) ng/ml; $p = 0.0282$] (Fig. 1A). These data suggest that although PBMCs from HVL subjects are abnormal in some way, PBMCs from LVL subjects are almost normal in terms of cytokine production.

As shown in Fig. 1A, mean cytokine levels were significantly lower in HVL subjects compared to LVL subjects, as follows: MIP-1α [6.33 (0.99-21.01) vs. 14.36 (2.29–29.16) ng/ml; $p = 0.0077$], MIP-1β [8.51 (1.37–26.42) vs. 20.14 (4.31–48.75) ng/ml; $p = 0.0034$], RANTES [2.01 (<0.015–4.57) vs. 3.40 (1.33–6.90) ng/ml; $p = 0.0014$], sIL-2R [2.30 (0.02–4.96) vs. 3.72 (1.72–7.38) ng/ml; $p = 0.0136$], IL-17 [0.04 (<0.01–0.12) vs. 0.08 (<0.01–0.17) pg/ml; $p = 0.0256$], and IL-7 [<0.01 (<0.01–0.67) vs. 0.05 (<0.01–1.05) pg/ml; $p = 0.0029$]. Notably, there was an inverse correlation between VL and production of these cytokines, and of IFN-γ (Fig. 1B). No relationship was observed between cytokine levels and CD4 cell count (data not shown). These data suggest that VL directly affects the capacity of PBMCs to produce certain cytokines during chronic infection.

Th1- and Th17-type T cells have impaired cytokine production in HVL subjects

Although PHA is considered a T cell mitogen, other cell populations also produce cytokines in response to PHA stimulation.[20–22] The next step was to determine which cells were responsible for the alterations in cytokine production observed under our experimental conditions. The cytokines whose production was inversely correlated with VL can be produced by several cell populations in PBMCs. To identify the major cell population producing these cytokines, we fractionated PBMCs in healthy donors by positive selection and determined the cell population producing these cytokines. $CD4^+$ T cells, $CD8^+$ T cells, monocytes ($CD14^+$), and NK cells ($CD56^+CD16^+$) were isolated from PBMCs, cultured separately or cocultured, and stimulated with PHA. We then measured levels of MIP-1α, MIP-1β, RANTES, IFN-γ, sIL-2R, and IL-17. Little or no production of these cytokines was detected in any of the single cell fractions (Fig. 2A). Production of cytokines MIP-1α, MIP-1β, RANTES, IFN-γ, and sIL-2R was observed in cocultures of $CD4^+$ and $CD14^+$ cells and in cocultures of $CD8^+$ and $CD14^+$ cells (Fig. 2A, and data not shown). IL-17 production was detected only in cocultures of $CD4^+$ and $CD14^+$ cells (Fig. 2A). As T cell stimulation by

TABLE 1. PATIENT CHARACTERISTICS

	Diagnosis (month)	*Sex*	*Age*	*VL*	*CD4*	*CD8*	*Treatment period (month)*
19 LVL							
S70	*9*	*M*	*47*	*53*	*481*	*746*	
T16	*60*	*F*	*41*	*240*	*492*	*804*	
O12	*61*	*M*	*32*	*450*	*559*	*1,187*	
S33	*125*	*M*	*52*	*470*	*400*	*888*	
K2	*60*	*M*	*30*	*510*	*316*	*871*	
M3	*160*	*F*	*34*	*730*	*444*	*859*	
S81	*6*	*M*	*32*	*1,700*	*381*	*1,475*	
Y1	*131*	*M*	*36*	*1,700*	*358*	*753*	
F4	*101*	*M*	*32*	*2,000*	*404*	*699*	
E6	*13*	*M*	*29*	*2,100*	*348*	*649*	
T24	30	M	46	400	455	469	
O16	23	M	36	1,100	362	812	
F9	65	M	35	1,100	517	1,066	
K11	33	M	30	1,200	521	1,137	
F1	41	M	35	1,600	424	1,151	
H25	6	M	43	1,700	749	821	
K16	61	F	23	2,000	560	1,049	
A10	32	M	25	3,400	586	1,603	
T26	28	M	36	3,600	449	864	
median	41		35	1,200	449	868	
16 HVL							
S60	*22*	*M*	*36*	*35,000*	*321*	*486*	
H24	*23*	*M*	*35*	*42,000*	*462*	*907*	
F13	*22*	*M*	*34*	*51,000*	*520*	*831*	
O29	*9*	*M*	*21*	*56,000*	*314*	*880*	
Y24	*14*	*M*	*25*	*58,000*	*381*	*2,023*	
K54	*10*	*M*	*24*	*82,000*	*386*	*1,056*	
K43	*11*	*M*	*29*	*110,000*	*361*	*507*	
S78	*5*	*M*	*48*	*260,000*	*492*	*1,441*	
K46	*15*	*M*	*47*	*280,000*	*454*	*1,579*	
S55	*26*	*M*	*56*	*500,000*	*427*	*510*	
T37	3	M	30	25,000	254	626	
K33	24	M	39	27,000	314	832	
M11	58	M	38	33,000	228	908	
O17	24	M	33	66,000	494	632	
T35	4	M	20	78,000	434	1,133	
S5	49	M	62	85,000	516	1,029	
median	18.5		35	62,000	407	894	
15 Tx							
U5	*22*	*M*	*42*	*30*	*308*	*581*	*22*
S19	*82*	*M*	*35*	*30*	*382*	*533*	*22*
T18	*70*	*M*	*40*	*40*	*508*	*747*	*66*
T8	*39*	*M*	*42*	*50*	*423*	*491*	*51*
K4	*73*	*M*	*31*	*50*	*480*	*718*	*71*
Y17	*33*	*M*	*36*	*50*	*365*	*508*	*31*
I9	*90*	*M*	*50*	*50*	*406*	*643*	*80*
I5	*59*	*M*	*44*	*50*	*466*	*668*	*56*
N11	*119*	*M*	*39*	*67*	*440*	*886*	*117*
N17	*60*	*M*	*29*	*67*	*382*	*571*	*46*
K24	150	M	54	40	610	805	149
N5	72	M	37	45	633	706	41
O9	61	M	41	50	335	629	72
Y5	81	M	36	110	753	605	79
S15	113	M	38	130	814	1,048	111
median	72		39	50	440	643	66

Italics indicates the patients used for phenotype and activation/exhaustion status of T cells.
VL, viral load; LVL, low viral load; HVL, high viral load; Tx, treatment experienced.

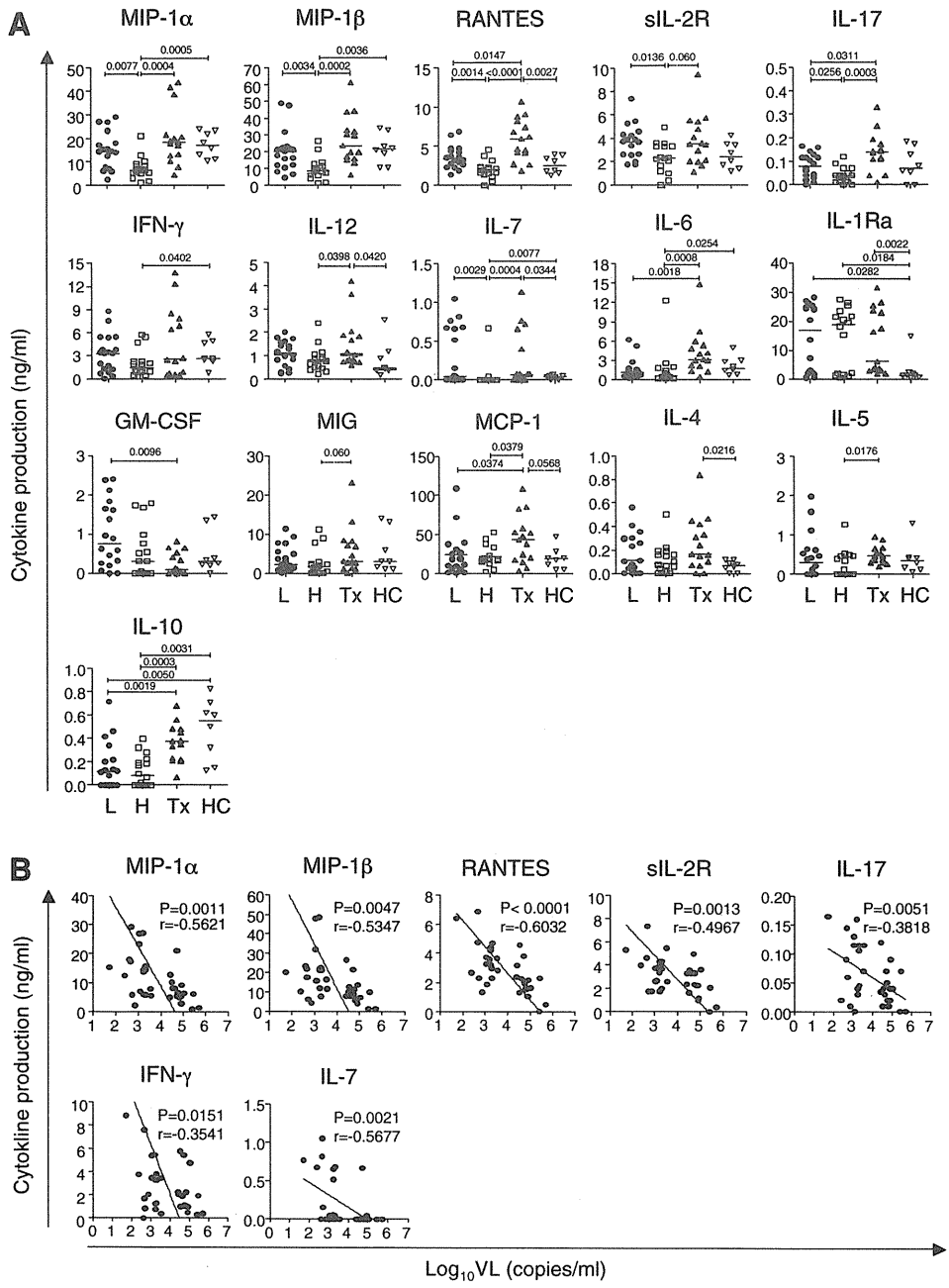

FIG. 1. Multiple cytokine production of phytohemagglutinin (PHA)-stimulated peripheral blood mononuclear cells (PBMCs) in chronic HIV-1-infected subjects and healthy individuals. **(A)** Comparison of cytokine production from PHA-stimulated PBMCs. L, LVL subjects (●), H, HVL subjects (□), Tx, HIV-1-infected subjects with prolonged antiretroviral therapy (ART) (▲), HC, healthy control (□). The horizontal bars indicate the median value. Differences between groups were tested for statistical significance by the Mann–Whitney *U* test. **(B)** Correlation between cytokine production and viral load. Correlation analysis was performed with Spearman's rank correlation to determine correlations between variables.

PHA requires accessory cells such as monocytes and macrophages,[23,24] these data indicate that $CD4^+$ and $CD8^+$ T cells are the sources of MIP-1α, MIP-1β, RANTES, IFN-γ, and sIL-2R production, and that only $CD4^+$ T cells are the source of IL-17.

$CD4^+$ T cells were classified into subsets based on cytokine secretion.[14,16] We found VL-associated reductions in levels of IFN-γ and IL-17 levels, which are typical cytokines secreted by Th1 and Th17 cells, respectively. In contrast, as shown in Fig. 1A, the LVL and HVL groups had comparable levels of IL-4, IL-5, and IL-13, which are associated with a Th2-type response, and IL-10, which is produced by regulatory T cells (Treg) (Fig. 1A). These results suggest that $CD4^+$ T cell dysfunction in HVL may occur in a type-specific manner, especially in Th1 and Th17 cells.

To determine which types of T cells could secrete MIP-1α, MIP-1β, and RANTES under our experimental conditions, we examined the expression pattern of MIP-1α/MIP-1β/RANTES, IFN-γ, and IL-17 by intracellular cytokine staining (ICS) after nonspecific T cell stimulation. Production of MIP-1α/MIP-1β/RANTES occurred in IFN-γ-expressing $CD4^+$ T cells, particularly in the subset of cells that expressed high levels of IFN-γ (Fig. 2B left). IL-17 was also produced in $CD4^+$ T cells, but was secreted by a different $CD4^+$ T cell subset. In $CD8^+$ T cells, most IFN-γ-expressing cells produced MIP-1α/MIP-1β/RANTES, and IL-17 was not produced at all (Fig. 2B right). Thus, our assays showed that MIP-1α, MIP-1β, and RANTES are secreted from Th1-type $CD4^+$ T cells and $CD8^+$ T cells, and that IL-17-secreting cells (Th17 cells) are clearly distinct. These data suggest that cytokine production by T

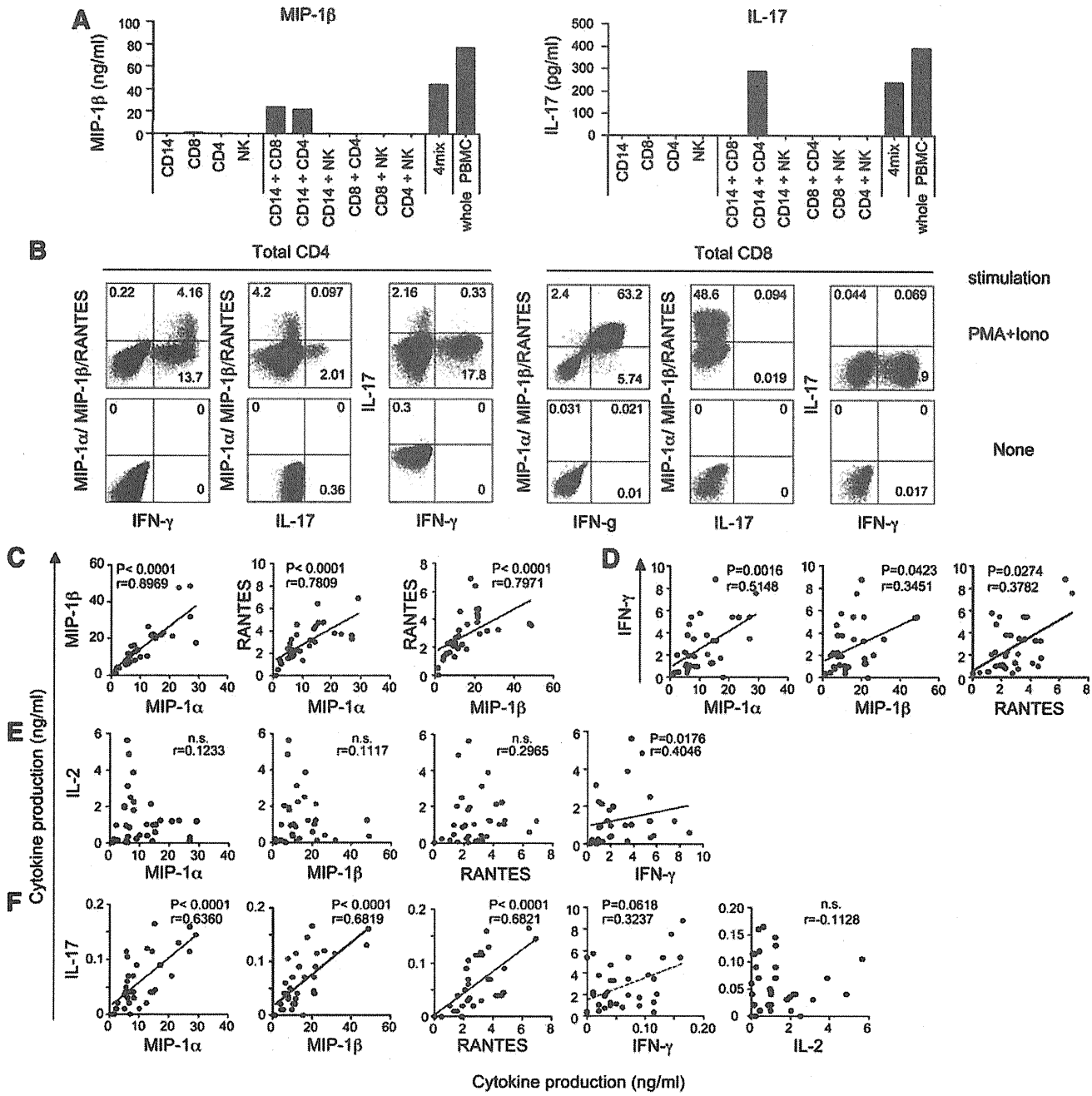

FIG. 2. Identification of cytokine-producing cells and relationships between cytokines. **(A)** Cytokine production in cell fractions from PBMCs. The results of MIP-1β and IL-17 production are shown. Fractionated $CD4^+$, $CD8^+$, $CD14^+$, and NK ($CD56^+CD16^+$) cells from PBMCs in healthy individuals were cultured separately or cocultured for 48 h after PHA stimulation. The experiment was repeated twice with PBMCs from different donors. **(B)** Representative flow cytometric analysis of intracellular cytokine staining for MIP-1α, MIP-1β, RANTES, IFN-γ (Th1 cytokine), and IL-17 after PMA/ionomycin stimulation in PBMCs of healthy individual. **(C–F)** Correlation between each cytokine production in treatment-naive HIV-1-infected subjects. MIP-1α, MIP-1β, and RANTES production **(C)**, IFN-γ production and MIP-1α, MIP-1β, or RANTES production **(D)**, IL-2 production and MIP-1α, MIP-1β, RANTES, or IFN-γ production **(E)**, IL-17 production and MIP-1α, MIP-1β, RANTES, IFN-γ, or IL-2 production **(F)** are shown. Correlation analysis was performed with Spearman's rank correlation to determine correlations between variables.

cells from the HVL group is dysfunctional, specifically in some of the Th1-related cytokines and in IL-17.

We next analyzed the correlation between production of Th1 cytokines (IFN-γ and IL-2), MIP-1α/MIP-1β/RANTES, and IL-17 in treatment-naive HIV-1 subjects. The levels of MIP-1α, MIP-1β, and RANTES showed strong positive correlations to each another (Fig. 2C), and correlations between IFN-γ and each of them were also significant (Fig. 2D). However, IL-2, another typical Th1 cytokine, did not show any significant correlation with MIP-1α, MIP-1β, and RANTES (Fig. 2E). Surprisingly, we found strong correlations between IL-17 production and MIP-1α/MIP-1β/RANTES

levels or IFN-γ levels, despite the fact that these cytokines are produced by different cells (Fig. 2F). These data suggest interrelated production of IFN-γ, MIP-1α, MIP-1β, RANTES, and IL-17 in T cells, but not of IL-2. Moreover, the capacity of T cells to produce these cytokines appears to be affected by HIV-1 VL *in vivo*.

Both central and effector memory CD4$^+$ and CD8$^+$ T cells are highly activated and exhausted in HVL subjects

The mechanism underlying the reduction in levels of specific cytokines in the HVL group could result either from decreased numbers of the cytokine-producing cells or from decreased productive capacity in those cells. We quantitated CD4$^+$ and CD8$^+$ T cells in HIV-1-infected patients (Table 1) and healthy control subjects (data not shown) by FACS. Although the number of CD4$^+$ T cells was significantly higher and the number of CD8$^+$ T cells significantly lower in HC than in HIV-positive patients, the differences in these T cell subsets were not significant between HVL and LVL.

As the number of monocytes seemed to affect T cell stimulation by PHA, we also analyzed monocytes (CD14$^+$ cells) and found there was no quantitative difference between any of the groups (data not shown).

As the cytokine productive capacity of T cells differs according to their differentiation status,[25] we explored the differentiation status of CD4$^+$ and CD8$^+$ T cells. We divided CD4$^+$ and CD8$^+$ T cells into four subsets depending on the expression pattern of CD45RA and CCR7: naive (CD45RA$^+$/CCR7$^+$), central memory (CM; CD45RA$^-$/CCR7$^+$), effector memory (EM; CD45RA$^-$/CCR7$^-$), and effector (CD45RA$^+$/CCR7$^-$) subsets. The proportion of each subset was highly heterogenic between subjects. The HVL and LVL subjects showed no significant differences in distribution of T cell subsets except in the proportion of naive CD8$^+$ T cells (data not shown), which cannot secrete cytokines even following PHA stimuli (Fig. 3A).[26]

To investigate whether there are qualitative differences in T cells between HVL and LVL subjects, we analyzed the expression of CD38, Ki67, Bcl2, PD-1, and CTLA-4 as markers of the activation and exhaustion status of T cells, which seems to affect their capacity to produce cytokines (Fig. 3B). In both CD4$^+$ and CD8$^+$ T cells, CM and EM subsets that mainly secrete these cytokines were highly activated (CD38$^+$, Ki67$^+$, and/or Bcl-2$^-$) in HVL subjects compared to LVL subjects (Fig. 3C). Especially in CM subsets of CD4$^+$ T cells, the frequency of exhausted cells (PD-1$^+$ and CTLA-4$^+$) was also significantly higher in HVL subjects compared to LVL subjects ($p < 0.05$ for both comparisons). EM subsets in CD4$^+$ T cells and CM and EM subsets in CD8$^+$ T cells also tended to be highly exhausted, although these differences were statistically insignificant in HVL subjects. These data indicate that memory CD4$^+$ and CD8$^+$ T cells, but not naive and effector subsets, are highly activated and exhausted in HVL subjects.

Poor cytokine production is directly correlated with activation/exhaustion status in memory T cells

As exhausted memory CD8$^+$ T cells fail to produce effector cytokines, such as IL-2, IFN-γ, and TNF-α, upon antigen stimulation,[27,28] we analyzed the relationship between the expression level of activation/exhaustion markers (CD38, Ki67, Bcl2, PD-1, and CTLA-4) on memory CD4$^+$ and CD8$^+$ T cells and the reduced production of cytokines seen in HVL subjects in response to PHA stimulation. The proportions of PD-1$^+$ and CD38$^+$ cells in CM subsets were inversely correlated with the capacity to produce MIP-1α, MIP-1β, RANTES, IFN-γ, and IL-17 (Fig. 4, and data not shown). In the EM subsets, proportions of PD-1$^+$ and CD38$^+$ cells, but not of CTLA4$^+$ cells, were inversely correlated with cytokine production. These data suggest that the compromised productive capacity of Th1-related and IL-17 cytokines is directly associated with persistent activation and exhaustion in memory T cells.

Cytokine production capacity is recovered soon after ART initiation, but memory CD8$^+$ T cells remain activated and exhausted even after prolonged viral suppression by ART

To explore whether the low cytokine production in HVL subjects is a cause or a consequence of high viral load, we compared cytokine production in subjects whose VL had been suppressed by ART for a prolonged period (>22 months) and whose CD4 count was at a similar level to that of HVL and LVL subjects (Tx subjects). In these subjects, production of the cytokines that were decreased in HVL subjects (MIP-1α, MIP-1β, RANTES, IFN-γ, sIL-2R, IL-7, and IL-17) was significantly higher than in HVL subjects, and production of MIP-1α, MIP-1β, sIL-2R, IL-7, and IFN-γ was at a similar level to that seen in LVL and HC subjects (Fig. 1A). Production of RANTES and IL-17 was higher in subjects with long-term viral suppression than in the other groups.

To clarify the relationship between VL and cytokine production capacity, we performed a similar analysis in subjects with dramatic reductions in VL due to recent ART initiation. We measured cytokine production from PBMCs isolated from blood drawn from six HIV-1-infected subjects within 1–2 months after starting ART, when VL had undergone dramatic reduction (mean VL=440 copies/ml, range 63 to 1100) (Fig. 5A). The levels of cytokines MIP-1α, MIP-1β, RANTES, and IL-7 produced after PHA stimulation were comparable to those seen in subjects with long-term suppression from ART (Fig. 5B). These data indicate that dysfunction of these cytokine production in individuals with high VL is reversible and is recovered soon after the VL reduction.

We also analyzed the activation and exhaustion status of CD4$^+$ and CD8$^+$ T cells in treatment-experienced (Tx) subjects (Fig. 3C). With the sole exception of CTLA-4 expression on the EM subset in CD8$^+$ T cells, proportions of activated (CD38$^+$, Ki67$^+$, and Bcl-2$^-$) cells and exhausted (PD-1$^+$ and CTLA-4$^+$) cells within both memory CD4$^+$ and CD8$^+$ T cell populations were significantly lower in Tx subjects compared to HVL subjects (Fig. 3C).

We next examined the activation/exhaustion status of memory CD4$^+$ and CD8$^+$ cells in Tx subjects compared to uninfected control subjects to determine whether the T cell status can revert to normal status after prolonged viral suppression by ART. The Tx and HC groups did not differ significantly in expression levels of markers in memory CD4$^+$ T cells (Fig. 3C). In contrast, the two groups differed significant in the activation/exhaustion status of memory CD8$^+$ T cells, with higher levels of Ki67, PD-1, and/or CTLA-4 expression and lower levels of Bcl-2 expression, in Tx subjects compared

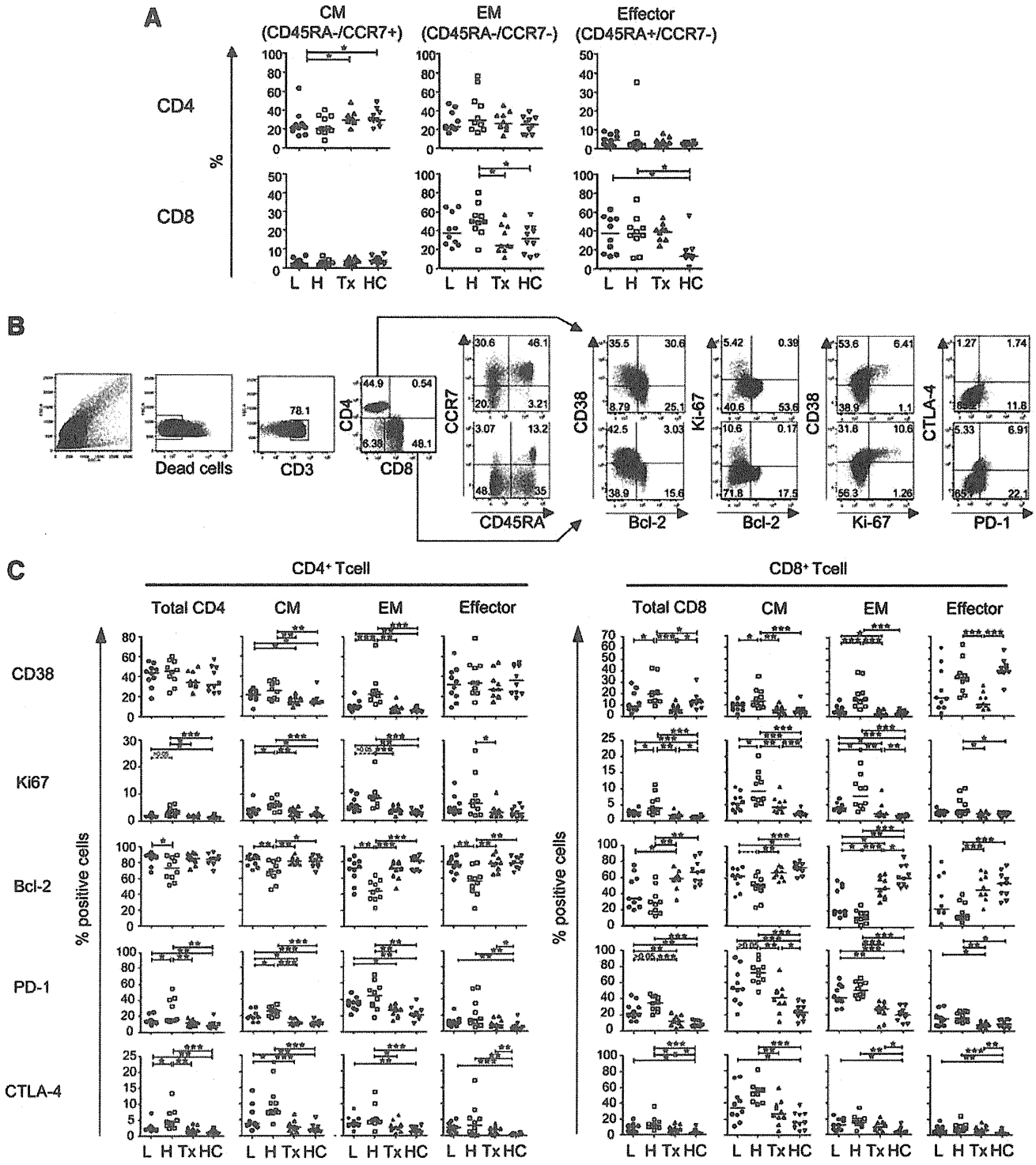

FIG. 3. Differentiation and activation/exhaustion status of $CD4^+$ and $CD8^+$ T cells in HIV-1-infected subjects. **(A)** Comparison of the frequency of $CD4^+$ and $CD8^+$ T cell subsets. The percentages of central memory (CM; $CD45RA^-/CCR7^+$), effector memory (EM; $CD45RA^-/CCR7^-$), and effector ($CD45RA^+/CCR7^-$) subsets in $CD4^+$ and $CD8^+$ T cells are shown. **(B)** Representative flow cytometric analysis of activation (CD38, Ki67, and Bcl2 expression) and exhaustion (PD-1 and CTLA-4 expression) status in $CD4^+$ and $CD8^+$ T cells. **(C)** Comparison of the activation/exhaustion status in $CD4^+$ and $CD8^+$ T cell subsets. L, LVL subjects (●), H, HVL subjects (□), Tx, HIV-1-infected subjects with prolonged ART (▲), HC, healthy control (□). The horizontal bars indicate the median value. Differences between groups were tested for statistical significance by the Mann–Whitney *U* test. $^*p = 0.01$ to 0.05, $^{**}p = 0.001$ to 0.01, $^{***}p < 0.001$ (Mann–Whitney test).

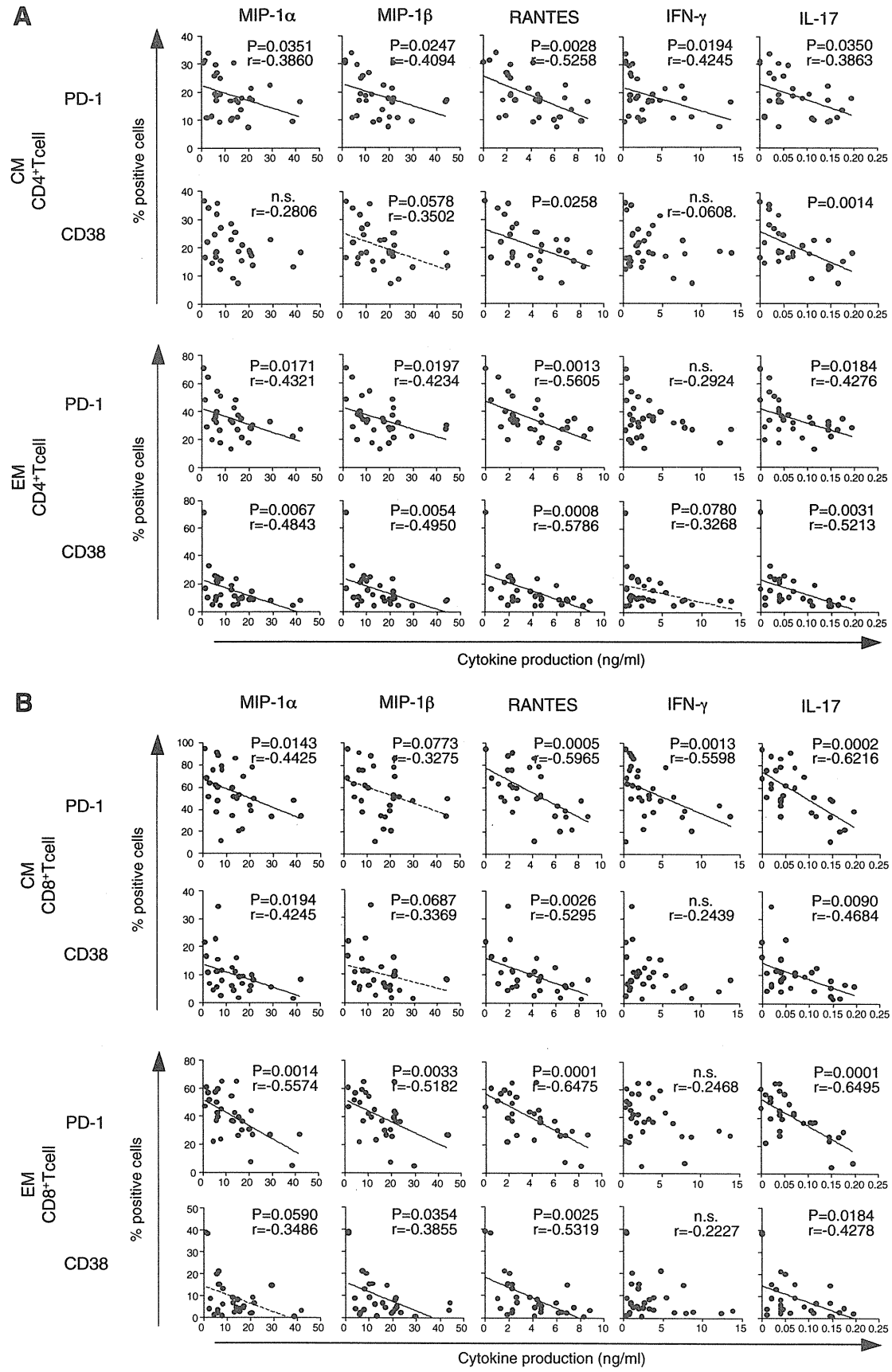

FIG. 4. Correlation between activation/exhaustion status in memory T cell subsets and cytokine production. Each panel indicates the relationship between the frequency of PD-1 or CD38 expressing cells in central memory (CM) and effector memory (EM) T cells and each cytokine production. The results of $CD4^+$ T cells and $CD8^+$ T cells are shown in **(A)** and **(B)**, respectively. Correlation analysis was performed with Spearman's rank correlation to determine correlations between variables.

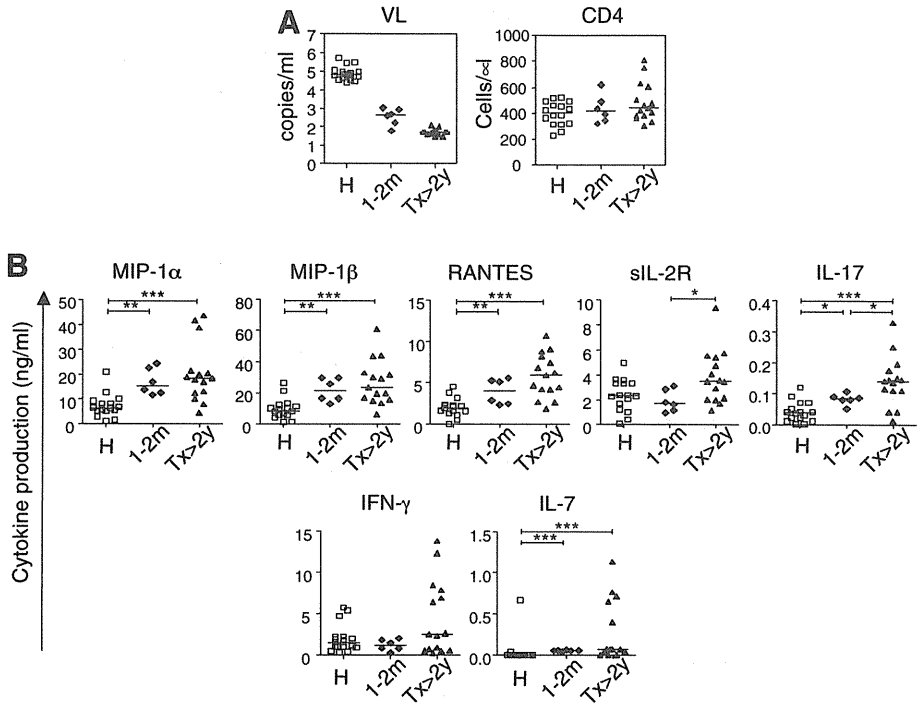

FIG. 5. Rapid recovery of cytokine production after initiation of antiretroviral therapy. **(A)** Viral load and CD4 count of each group. **(B)** Comparison of cytokine production by PHA-stimulated PBMCs. H, HVL subjects (□), 1–2 months, subjects 1–2 months after starting ART (□), Tx > 2 years, subjects with prolonged ART (▲). $^{*}p = 0.01$ to 0.05, $^{**}p = 0.001$ to 0.01, $^{***}p < 0.001$ (Mann–Whitney test).

to HC subjects. These data suggest that although suppression of HIV-1 replication by ART dramatically improves the cytokine production capacity of T cells to a normal level, memory $CD8^+$ T cells, but not memory $CD4^+$ T cells, remain somewhat activated even after prolonged viral suppression.

Discussion

Despite intensive research, it remains unclear how HIV-1 can cause the collapse of the host immune system and development of AIDS after chronic infection. In this study, we demonstrate that high HIV-1 viral load associates with skewed T cell dysfunction in cytokine production, independently of CD4 T cell count. Diminished cytokine production in subjects with high VL is specific for some Th1-related cytokines (MIP1-α, MIP-1β, RANTES, and IFN-γ), IL-17, IL-7, and sIL-2R, and is associated with activation and exhaustion status in both $CD4^+$ and $CD8^+$ T cells, especially in memory subsets. The dysfunctional production of these cytokines in HVL subjects appears to be reversible, with recovery occurring after VL reduction by ART.

In this study, we tried to find as many cytokines as possible that differ between LVL and HVL subjects. For this reason, we used a strong stimulus and long incubation times to show the results clearly. The 48-h culture period is long enough to allow expression both of late-response genes and of secondary response genes that may be induced following the primary response.

Production of MIP-1α, MIP-1β, and RANTES was dramatically reduced in HVL subjects and showed a close inverse correlation with plasma VL (Fig. 1). As the natural ligands of HIV-1 coreceptor CCR5, MIP-1α/MIP-1β/RANTES are potent inhibitors of CCR5-tropic HIV-1 (R5-HIV-1) infection.[29] Physiologically, these chemokines also play a key role in induction of cellular immune responses by recruiting $CCR5^+$ Th1 lymphocytes to the infectious site *in vivo*.[30–33] In the case of HIV-1 infection, decreased production of these chemokines seems to favor both viral expansion and reduced migration of effector T cells *in vivo*. In recent studies, a high copy number of CCL3L1 (one of the genes encoding MIP-1α) combined with a low CCR5 expression genotype was associated with low VL in HIV-1-infected subjects,[34,35] suggesting that CCL3L1-CCR5 genotypes may be able to modify the clinical course of HIV-1 infection.

In our study plasma VL affected the ability of T cells to produce IFN-γ, one of the cytokines that defines Th1 cells, and IL-17, which is a Th17-type cytokine. However, no effect was seen on Th2-type cytokines (IL-4, IL-5, and IL-13) or IL-10. Interferon-γ, MIP-1α, MIP-1β,and RANTES are produced by Th1 cells (Fig. 2B), which preferentially express CCR5,[30] and Th17 cells are known to express CCR5 in peripheral blood.[36,37] However, Th2 cells do not express CCR5.[30] Transcription of these cytokines in T cells may be influenced by CCR5 signaling. Large amounts of R5-HIV-1 or the Env protein might persistently trigger the signaling pathway by binding to CCR5, thereby causing reductions in levels of specific cytokines in chronically HIV-1 subjects.

In our experiments, MIP-1α, MIP-1β, and RANTES were produced by IFN-γ-expressing cells in subsets of $CD4^+$ and $CD8^+$ T cells, and IL-17 was produced by a different subset of $CD4^+$ T cells. Surprisingly, IL-17 production was strongly correlated with MIP-1α, MIP-1β, RANTES, and IFN-γ production even though the producer cells are different (Fig. 2F). This correlation might reflect a general ability of Th1 and Th17 cells to produce cytokines. However, IL-2 production was not correlated with MIP-1α, MIP-1β, RANTES, and IFN-γ production, despite the fact that IL-2 should be produced by the same IFN-γ-producing cells (Fig. 2C–F). Critical regions of IFN-γ promoter (i.e., consensus GATA motif and essential functional motif) are not found in the IL-2 promoter region, but are found in the MIP-1α and MIP-1β promoters.[38] In addition, the same sequence in the promoter region of IFN-γ,

MIP-1α, and MIP-1β was found in the IL-17 promoter.[39] Interferon-γ, MIP-1α, MIP-1β, RANTES, and IL-17 production in T cells may be coordinately regulated, and the productive capacity of these cytokines appears to be affected by HIV-1 VL in a similar fashion. Alternatively, we measured cytokine production 48 h after PHA stimulation in this study. The period is long enough to develop sequential reactions occurring in response to primary reaction. As IFN-γ is known as an early-response gene and has the potential to affect multiple immune responses,[40] the production of MIP-1α, MIP-1β, RANTES, and IL-17, but not IL-2 may depend on the amount of IFN-γ as the primary response. Further studies are required to elucidate the mechanism by which IL-17 production is correlated with MIP-1α, MIP-1β, RANTES, or IFN-γ production. The IFN-γ pathway protects against intracellular pathogens through cellular immunity, and IL-17 provides protection against extracellular pathogens and fungal infections.[41,42] Although their target pathogens differ, IL-17 regulates the Th1 immune response through IL-17 receptor-expressing dendritic cells (DC) and macrophages.[43] These data suggest that Th1-type and Th17-type immune responses are closely related, and that their interaction is crucial for immune protection.

In a pathogenic SIV infection model, the loss of Th17 cells in the gastrointestinal tract dampens the intestinal mucosal barrier, resulting in microbial translocation, which in turn induces systemic immune activation.[44–47] In SIV infection the loss of Th17 cells in intestinal mucosa and in PBMCs is inversely correlated with plasma VL.[48] In this study, we observed a strong inverse correlation between IL-17 production and the proportion of activated and exhausted memory T cells. Our results suggest that not only the number of IL-17-producing cells but also the quality of those cells may account for the dysfunction of the Th17-type immune response in HVL subjects.

During chronic HIV-1 infection expression of the inhibitory coreceptors PD-1 and CTLA-4 on total T cells (not only HIV-1-specific T cells) is associated with plasma VL and CD4 count.[11,12] In this study, we found that the proportions of PD-1^+, $CTLA4^+$, and $CD38^+$ cells in total memory subsets of $CD4^+$ and $CD8^+$ T cells were inversely correlated with the ability of T cells to produce MIP-1α, MIP-1β, RANTES, IFN-γ, sIL-2R, and IL-17 in response to PHA stimulation (Fig. 4). It has been reported that PD-1 expression depends on the status of activation markers such as CD38 and on the differentiation stage of T cells.[49,50] Other studies have shown that blocking the pathway of the PD-1/PD-L1 interaction augments the cytokine production capacity of HIV-1-specific $CD4^+$ and $CD8^+$ T cells *in vitro*.[11,51] In our study, prolonged virus suppression by ART resulted in cytokine production capacities returning to normal (Fig. 1A). Memory subsets of $CD4^+$ T cells were no longer activated and exhausted (Fig. 3C), although memory subsets of $CD8^+$ T cells remained slightly activated/exhausted. These data suggest that activation and/or exhaustion of T cells is directly associated with the ability to produce these specific cytokines and that the impairment in T cell function is reversible.

Our study is the first to show that the T cell impairment in high VL subjects is specific for production of some of Th1-type and Th17-type cytokines, and that production of these cytokines is strongly correlated with one another. In subjects with high VL, a vicious cycle occurs, as T cells increasingly lose the capacity to produce these important cytokines. Notably, we also found that subjects who maintain a low VL, yet who are not "elite controllers," are capable of producing normal levels of these cytokines. These findings could be useful in guiding the development of new therapies focusing on immune control to reduce T cell activation in chronic HIV-1 infection.

Acknowledgments

We thank Nobukazu Watanabe for his technical advice and helpful discussion. This work was supported by a Grant-in-Aid for Scientific Research (C) (22590412) from the Japan Society for the Promotion of Science (JSPS), Grants for AIDS research from the Ministry of Health, Labor, and Welfare of Japan.

Author Disclosure Statement

No competing financial interests exist.

References

1. Mellors JW, Munoz A, Giorgi JV, *et al.*: Plasma viral load and CD4+ lymphocytes as prognostic markers of HIV-1 infection. Ann Intern Med 1997;126:946–954.
2. Grossman Z, Meier-Schellersheim M, Paul WE, and Picker LJ: Pathogenesis of HIV infection: What the virus spares is as important as what it destroys. Nat Med 2006;12:289–295.
3. Liu Z, Cumberland WG, Hultin LE, Prince HE, Detels R, and Giorgi JV: Elevated CD38 antigen expression on CD8+ T cells is a stronger marker for the risk of chronic HIV disease progression to AIDS and death in the Multicenter AIDS Cohort Study than CD4+ cell count, soluble immune activation markers, or combinations of HLA-DR and CD38 expression. J Acquir Immune Defic Syndr Hum Retrovirol 1997;16:83–92.
4. Silvestri G, Sodora DL, Koup RA, *et al.*: Nonpathogenic SIV infection of sooty mangabeys is characterized by limited bystander immunopathology despite chronic high-level viremia. Immunity 2003;18:441–452.
5. Hirsch VM: What can natural infection of African monkeys with simian immunodeficiency virus tell us about the pathogenesis of AIDS? AIDS Rev 2004;6:40–53.
6. Betts MR, Nason MC, West SM, *et al.*: HIV nonprogressors preferentially maintain highly functional HIV-specific CD8+ T cells. Blood 2006;107:4781–4789.
7. Freel SA, Lamoreaux L, Chattopadhyay PK, *et al.*: Phenotypic and functional profile of HIV-inhibitory CD8 T cells elicited by natural infection and heterologous prime/boost vaccination. J Virol 2010;84:4998–5006.
8. Nemes E, Bertoncelli L, Lugli E, *et al.*: Cytotoxic granule release dominates gag-specific CD4+ T-cell response in different phases of HIV infection. AIDS 2010;24:947–957.
9. Brenchley JM, Karandikar NJ, Betts MR, *et al.*: Expression of CD57 defines replicative senescence and antigen-induced apoptotic death of CD8+ T cells. Blood 2003;101:2711–2720.
10. Palmer BE, Blyveis N, Fontenot AP, and Wilson CC: Functional and phenotypic characterization of CD57+ CD4+ T cells and their association with HIV-1-induced T cell dysfunction. J Immunol 2005;175:8415–8423.
11. Day CL, Kaufmann DE, Kiepiela P, *et al.*: PD-1 expression on HIV-specific T cells is associated with T-cell exhaustion and disease progression. Nature 2006;443:350–354.
12. Kaufmann DE, Kavanagh DG, Pereyra F, *et al.*: Upregulation of CTLA-4 by HIV-specific CD4+ T cells correlates with

disease progression and defines a reversible immune dysfunction. Nat Immunol 2007;8:1246–1254.
13. D'Souza M, Fontenot AP, Mack DG, *et al.:* Programmed death 1 expression on HIV-specific CD4+ T cells is driven by viral replication and associated with T cell dysfunction. J Immunol 2007;179:1979–1987.
14. Mosmann TR and Coffman RL: TH1 and TH2 cells: Different patterns of lymphokine secretion lead to different functional properties. Annu Rev Immunol 1989;7:145–173.
15. Barrat FJ, Cua DJ, Boonstra A, *et al.:* In vitro generation of interleukin 10-producing regulatory CD4(+) T cells is induced by immunosuppressive drugs and inhibited by T helper type 1 (Th1)- and Th2-inducing cytokines. J Exp Med 2002;195:603–616.
16. Harrington LE, Hatton RD, Mangan PR, *et al.:* Interleukin 17-producing CD4+ effector T cells develop via a lineage distinct from the T helper type 1 and 2 lineages. Nat Immunol 2005;6:1123–1132.
17. Charlton B and Lafferty KJ: The Th1/Th2 balance in autoimmunity. Curr Opin Immunol 1995;7:793–798.
18. Clerici M and Shearer GM: A TH1→TH2 switch is a critical step in the etiology of HIV infection. Immunol Today 1993;14:107–111.
19. Thobakgale CF, Streeck H, Mkhwanazi N, *et al.:* CD8(+) T cell polyfunctionality profiles in progressive and nonprogressive pediatric HIV type 1 infection. AIDS Res Hum Retroviruses 2011;27:1005–1012.
20. Hammarstrom S, Hammarstrom ML, Sundblad G, Arnarp J, and Lonngren J: Mitogenic leukoagglutinin from Phaseolus vulgaris binds to a pentasaccharide unit in N-acetyllactosamine-type glycoprotein glycans. Proc Natl Acad Sci USA 1982;79:1611–1615.
21. Janossy G, Greaves MF, Doenhoff MJ, and Snajdr J: Lymphocyte activation. V. Quantitation of the proliferative responses to mitogens using defined T and B cell populations. Clin Exp Immunol 1973;14:581–596.
22. Scott MG and Nahm MH: Mitogen-induced human IgG subclass expression. J Immunol 1984;133:2454–2460.
23. Ceuppens JL, Baroja ML, Lorre K, Van Damme J, and Billiau A: Human T cell activation with phytohemagglutinin. The function of IL-6 as an accessory signal. J Immunol 1988;141:3868–3874.
24. Unanue ER and Allen PM: The basis for the immunoregulatory role of macrophages and other accessory cells. Science 1987;236:551–557.
25. Sallusto F, Lenig D, Forster R, Lipp M, and Lanzavecchia A: Two subsets of memory T lymphocytes with distinct homing potentials and effector functions. Nature 1999;401:708–712.
26. Agarwal S, Viola JP, and Rao A: Chromatin-based regulatory mechanisms governing cytokine gene transcription. J Allergy Clin Immunol 1999;103:990–999.
27. Wherry EJ and Ahmed R: Memory CD8 T-cell differentiation during viral infection. J Virol 2004;78:5535–5545.
28. Wherry EJ, Blattman JN, Murali-Krishna K, van der Most R, and Ahmed R: Viral persistence alters CD8 T-cell immunodominance and tissue distribution and results in distinct stages of functional impairment. J Virol 2003;77:4911–4927.
29. Cocchi F, DeVico AL, Garzino-Demo A, Arya SK, Gallo RC, and Lusso P: Identification of RANTES, MIP-1 alpha, and MIP-1 beta as the major HIV-suppressive factors produced by CD8+ T cells. Science 1995;270:1811–1815.
30. Bonecchi R, Bianchi G, Bordignon PP, *et al.:* Differential expression of chemokine receptors and chemotactic responsiveness of type 1 T helper cells (Th1s) and Th2s. J Exp Med 1998;187:129–134.
31. Ferbas J, Giorgi JV, Amini S, *et al.:* Antigen-specific production of RANTES, macrophage inflammatory protein (MIP)-1alpha, and MIP-1beta in vitro is a correlate of reduced human immunodeficiency virus burden in vivo. J Infect Dis 2000;182:1247–1250.
32. Siveke JT and Hamann A: T helper 1 and T helper 2 cells respond differentially to chemokines. J Immunol 1998;160: 550–554.
33. Taub DD, Conlon K, Lloyd AR, Oppenheim JJ, and Kelvin DJ: Preferential migration of activated CD4+ and CD8+ T cells in response to MIP-1 alpha and MIP-1 beta. Science 1993;260:355–358.
34. Dolan MJ, Kulkarni H, Camargo JF, *et al.:* CCL3L1 and CCR5 influence cell-mediated immunity and affect HIV-AIDS pathogenesis via viral entry-independent mechanisms. Nat Immunol 2007;8:1324–1336.
35. Gonzalez E, Kulkarni H, Bolivar H, *et al.:* The influence of CCL3L1 gene-containing segmental duplications on HIV-1/AIDS susceptibility. Science 2005;307:1434–1440.
36. Gosselin A, Monteiro P, Chomont N, *et al.:* Peripheral blood CCR4+ CCR6+ and CXCR3+ CCR6+ CD4+ T cells are highly permissive to HIV-1 infection. J Immunol 2010;184: 1604–1616.
37. Lim HW, Lee J, Hillsamer P, and Kim CH: Human Th17 cells share major trafficking receptors with both polarized effector T cells and FOXP3+ regulatory T cells. J Immunol 2008; 180:122–129.
38. Fernandez N, Renedo M, Garcia-Rodriguez C, and Sanchez Crespo M: Activation of monocytic cells through Fc gamma receptors induces the expression of macrophage-inflammatory protein (MIP)-1 alpha, MIP-1 beta, and RANTES. J Immunol 2002;169:3321–3328.
39. Dodon MD, Li Z, Hamaia S, and Gazzolo L: Tax protein of human T-cell leukaemia virus type 1 induces interleukin 17 gene expression in T cells. J Gen Virol 2004;85:1921–1932.
40. Penix L, Weaver WM, Pang Y, Young HA, and Wilson CB: Two essential regulatory elements in the human interferon gamma promoter confer activation specific expression in T cells. J Exp Med 1993;178:1483–1496.
41. Acosta-Rodriguez EV, Rivino L, Geginat J, *et al.:* Surface phenotype and antigenic specificity of human interleukin 17-producing T helper memory cells. Nat Immunol 2007;8:639–646.
42. Ouyang W, Kolls JK, and Zheng Y: The biological functions of T helper 17 cell effector cytokines in inflammation. Immunity 2008;28:454–467.
43. Lin Y, Ritchea S, Logar A, *et al.:* Interleukin-17 is required for T helper 1 cell immunity and host resistance to the intracellular pathogen Francisella tularensis. Immunity 2009;31: 799–810.
44. Brenchley JM, Price DA, Schacker TW, *et al.:* Microbial translocation is a cause of systemic immune activation in chronic HIV infection. Nat Med 2006;12:1365–1371.
45. Raffatellu M, Santos RL, Verhoeven DE, *et al.:* Simian immunodeficiency virus-induced mucosal interleukin-17 deficiency promotes Salmonella dissemination from the gut. Nat Med 2008;14:421–428.
46. Brenchley JM, Paiardini M, Knox KS, *et al.:* Differential Th17 CD4 T-cell depletion in pathogenic and nonpathogenic lentiviral infections. Blood 2008;112:2826–2835.
47. Brenchley JM and Douek DC: HIV infection and the gastrointestinal immune system. Mucosal Immunol 2008;1:23–30.
48. Cecchinato V, Trindade CJ, Laurence A, *et al.:* Altered balance between Th17 and Th1 cells at mucosal sites predicts

AIDS progression in simian immunodeficiency virus-infected macaques. Mucosal Immunol 2008;1:279–288.
49. Appay V, van Lier RA, Sallusto F, and Roederer M: Phenotype and function of human T lymphocyte subsets: Consensus and issues. Cytometry A 2008;73(11):975–983.
50. Sauce D, Almeida JR, Larsen M, *et al.:* PD-1 expression on human CD8 T cells depends on both state of differentiation and activation status. AIDS 2007;21:2005–2013.
51. Trautmann L, Janbazian L, Chomont N, *et al.:* Upregulation of PD-1 expression on HIV-specific CD8+ T cells leads to reversible immune dysfunction. Nat Med 2006;12: 1198–1202.

Address correspondence to:
Ai Kawana-Tachikawa
Division of Infectious Diseases
Advanced Clinical Research Center
The Institute of Medical Science
The University of Tokyo
4-6-1 Shirokanedai
Minato-ku
Tokyo 108-8639
Japan

E-mail: aikawana@ims.u-tokyo.ac.jp

ELSEVIER

INSTITUT PASTEUR

Microbes and Infection 13 (2011) 339–349

www.elsevier.com/locate/micinf

Original article

Huwe1, a novel cellular interactor of Gag-Pol through integrase binding, negatively influences HIV-1 infectivity

Seiji P. Yamamoto [a,b], Katsuya Okawa [c,1], Takashi Nakano [d], Kouichi Sano [d], Kanako Ogawa [e], Takao Masuda [f], Yuko Morikawa [g], Yoshio Koyanagi [a], Youichi Suzuki [e,*]

[a] *Laboratory of Viral Pathogenesis, Institute for Virus Research, Kyoto University, 53 Shogoin-kawahara-cho, Sakyo-ku, Kyoto 606-8507, Japan*
[b] *Department of Molecular and Cellular Biology, Graduate School of Biostudies, Kyoto University, Yoshida-konoe-cho, Sakyo-ku, Kyoto 606-8501, Japan*
[c] *Frontier Technology Center, Graduate School of Medicine, Kyoto University, Yoshida-konoe-cho, Sakyo-ku, Kyoto 606-8501, Japan*
[d] *Department of Microbiology and Infection Control, Osaka Medical College, 2-7 Daigaku-machi, Takatsuki, Osaka 569-8686, Japan*
[e] *Laboratory for Host Factors, Center for Emerging Virus Research, Institute for Virus Research, Kyoto University, 53 Shogoin-kawahara-cho, Sakyo-ku, Kyoto 606-8507, Japan*
[f] *Department of Immunotherapeutics, Graduate School of Medicine and Dentistry, Tokyo Medical and Dental University, 1-5-45 Yushima, Bunkyo-ku, Tokyo 113-8519, Japan*
[g] *Graduate School for Infection Control, Kitasato University, 5-9-1 Shirokane, Minato-ku, Tokyo 108-8641, Japan*

Received 11 October 2010; accepted 7 December 2010
Available online 15 December 2010

Abstract

Integration, an indispensable step for retrovirus replication, is executed by integrase (IN), which is expressed as a part of a Gag-Pol precursor. Although mechanistic detail of the IN-catalyzed integration reaction is well defined, numerous evidence have demonstrated that IN is involved in multiple steps of retrovirus replication other than integration. In this study, Huwe1, a HECT-type E3 ubiquitin ligase, was identified as a new cellular interactor of human immunodeficiency virus type 1 (HIV-1) IN. The interaction was mediated through the catalytic core domain of IN and a wide-range region of Huwe1. Interestingly, although depletion of Huwe1 in target cells did not affect the early phase of HIV-1 infection in a human T cell line, we found that infectivity of HIV-1 released from the Huwe1 knockdown cells was significantly augmented more than that of virus produced from control cells. The increase in infectivity occurred in proviral DNA synthesis. Further analysis revealed that Huwe1 interacted with HIV-1 Gag-Pol precursor protein through an IN domain. Our results suggest that Huwe1 in HIV-1 producer cells has a negative impact on early post-entry events during the next round of virus infection via association with an IN region of Gag-Pol.

Keywords: HIV-1; MoMLV; Integrase; Huwe1; Gag-Pol precursor protein

1. Introduction

An infecting retroviral virion contains genomic RNA together with viral proteins that are required for completing the early phase of infection. Following entry into the host cell, a copy of viral DNA is synthesized from the viral genome by its reverse transcriptase (RT) and, subsequently, integrated into chromosomal DNA to form provirus by the preintegration complex (PIC). This integration step is essential for retroviral replication and is catalyzed by a viral enzyme, integrase (IN). Retroviral IN consists of three structurally and functionally distinct domains called the N-terminal domain (NTD), catalytic core domain (CCD), and C-terminal domain (CTD) [1]. CCD is highly conserved amongst retroviral INs and contains the triad of conserved amino acids that comprise Asp, Asp, and Glu residues termed the D, D-35-E motif. This domain possesses a key role during the integration reaction [1]. A well-conserved motif is also

* Corresponding author. Present address: Department of Microbiology, Yong Loo Lin School of Medicine, National University of Singapore, 5 Science Drive 2, Blk MD4A, level 5, Singapore 117597, Singapore. Tel.: +65 6516 3484; fax: +65 6776 6872.
E-mail address: micys@nus.edu.sg (Y. Suzuki).
[1] Present address: Drug Discovery Research Laboratories, Kyowa Hakko Kirin Co., Ltd., Mishima, Shizuoka 411-8731, Japan.

1286-4579/$ - see front matter © 2010 Institut Pasteur. Published by Elsevier Masson SAS. All rights reserved.
doi:10.1016/j.micinf.2010.12.002